pared to glycine betaine induced the dissociation of the hexamer. Moreover, there was no effect of glycine betaine on the structural change of $ClpB_{Tha}$ under heat stress conditions (Fig. 5). Taken together, our observations indicate that the ATP-induced oligomerization of $ClpB_{Tha}$ was affected by the surrounding environmental conditions, such as a high temperature and the salt concentration.

Disaggregation activities are widely conserved among the ClpB homologs. In fact, $ClpB_{Tha}$ also reactivated heat-aggregated LDH in an ATP-dependent cooperation with the $DnaK_{Tha}$ system (Fig. 3). Interestingly, $ClpB_{Tha}$ exhibited general chaperone activities, such as the protection of substrates from both thermal inactivation and aggregation, in the absence of ATP (Fig. 4). Under these conditions, as demonstrated by cross-linking (Fig. 2A), $ClpB_{Tha}$ formed dimers and monomers. After the dissociation of the hexamer into dimers and monomers, these species appear to expose the hydrophobic regions and substrate binding sites hidden inside the ring; this might enable the molecules to interact with unfolded proteins. This behavior may be similar to that of other chaperones, including the DnaK and GroEL systems. Why, nevertheless, does $ClpB_{Tha}$ possess intrinsic chaperone activities? One possible explanation is that $ClpB_{Tha}$ compensates for the impaired function of the $DnaK_{Tha}$ system whose in vitro chaperone activity is lower than that of the *E. coli* system (S. Sugimoto et al., unpublished data). The independent and/or cooperative functions of the $ClpB_{Tha}$ and $DnaK_{Tha}$ systems are now under investigation in vivo.

Based on the results presented in this study, we propose the following model for the structural and functional conversion of $ClpB_{Tha}$ (data not shown). Under stress conditions, particularly at high temperatures, intracellular labile proteins might be easily denatured and form aggregates. Accumulations of large amounts of these aggregates and the loss of active proteins, including several essential for cell growth, have toxic effects on the host cells (32). Under these types of stress conditions, $ClpB_{Tha}$ forms dimer and monomer structures and these protect substrate proteins from aggregation by binding to unfolded proteins and by suppressing the formation of aggregates. This facilitates a rapid first defense against stress, including heat and salt stress. Under poststress conditions, aggregates formed in response to stress would be repaired by the DnaK-ClpB bichaperone system, where $ClpB_{Tha}$ forms hexameric ring structure depending on the presence of ATP.

To our knowledge, this is the first report to describe the functional conversion of the molecular chaperone ClpB associated with a structural change. Further investigations will be required to determine whether this property is common among gram-positive bacteria and some other organisms; these investigations may provide us with a unique insight into the role of molecular chaperone systems.

ACKNOWLEDGMENTS

We thank Akemi Takade (Department of Bacteriology, Faculty of Medical Science, Graduate School, Kyushu University, Japan) for the electron microscopy. We appreciate Mitsuru Abo (Department of Applied Biological Chemistry, Graduate School of Agricultural and Life Sciences, The University of Tokyo, Japan) for the quantification of intracellular ionic concentrations. We gratefully acknowledge Toshifumi Tomoyasu (Department of Microbiology and Molecular Genetics, Graduate School of Pharmaceutical Sciences, Chiba University, Japan) for helpful discussions on this study.

This work was supported in part by a grant of the JSPS Research Fellowship (0166799) for young scientists.

REFERENCES

1. **Akoev, V., E. P. Gogol, M. E. Barnett, and M. Zolkiewski.** 2004. Nucleotide-induced switch in oligomerization of the AAA^+ ATPase ClpB. Protein Sci. **13**:567–574.
2. **Barnett, M. E., A. Zolkiewska, and M. Zolkiewski.** 2000. Structure and activity of ClpB from *Escherichia coli*. Role of the amino- and carboxyl-terminal domains. J. Biol. Chem. **275**:37565–37571.
3. **Beinker, P., S. Schlee, Y. Groemping, R. Seidel, and J. Reinstein.** 2002. The N terminus of ClpB from *Thermus thermophilus* is not essential for the chaperone activity. J. Biol. Chem. **277**:47160–47166.
4. **Chastanet, A., I. Derré, S. Nair, and T. Msadek.** 2004. *clpB*, a novel member of the *Listeria monocytogenes* CtsR regulon, is involved in virulence but not in general stress tolerance. J. Bacteriol. **186**:1165–1174.
5. **Collins, M. D., A. M. Williams, and S. Wallbanks.** 1990. The phylogeny of *Aerococcus* and *Pediococcus* as determined by 16S rRNA sequence analysis: description of *Tetragenococcus* gen. nov. FEMS Microbiol. Lett. **70**:255–262.
6. **Derré, I, G. Rapoport, and T. Msadek.** 1999. CtsR, a novel regulator of stress and heat shock response, controls *clp* and molecular chaperone gene expression in gram-positive bacteria. Mol. Microbiol. **31**:117–131.
7. **Diamant, S., D. Rosenthal, A. Azem, N. Eliahu, A. P. Ben-zi, and P. Goloubinoff.** 2003. Dicarboxylic amino acids and glycine-betaine regulate chaperone-mediated protein-disaggregation under stress. Mol. Microbiol. **49**:401–410.
8. **Ekaza, E., J. Teyssier, S. Ouahrani-Bettache, J. P. Liautard, and S. Köhler.** 2001. Characterization of *Brucella suis clpB* and *clpAB* mutants and participation of the genes in stress responses. J. Bacteriol. **183**:2677–2681.
9. **Eriksson, M. J., and A. K. Clarke.** 1996. The heat shock protein ClpB mediates the development of thermotolerance in the cyanobacterium *Synechococcus sp.* strain PCC 7942. J. Bacteriol. **178**:4839–4846.
10. **Fukuda, D., M. Watanabe, S. Sonezaki, S. Sugimoto, K. Sonomoto, and A. Ishizaki.** 2002. Molecular characterization and regulatory analysis of *dnaK* operon of halophilic lactic acid bacterium *Tetragenococcus halophila*. J. Biosci. Bioeng. **93**:388–394.
11. **Glover, J. R., and S. Lindquist.** 1998. Hsp104, Hsp70, and Hsp40: a novel chaperone system that rescues previously aggregated proteins. Cell **94**:73–82.
12. **Goloubinoff, P., A. Mogk, A. P. B. Zvi, T. Tomoyasu, and B. Bukau.** 1999. Sequential mechanism of solubilization and refolding of stable protein aggregates by a bichaperone network. Proc. Natl. Acad. Sci. USA **96**:13732–13737.
13. **Ingmer, H., F. K. Vogensen, K. Hammer, and M. Kilstrup.** 1999. Disruption and analysis of the *clpB*, *clpC*, and *clpE* genes in *Lactococcus lactis*: ClpE, a new Clp family in gram-positive bacteria. J. Bacteriol. **181**:2075–2083.
14. **Kim, K. I., G. W. Cheong, S. C. Park, J. S. Ha, K. M. Woo, S. J. Choi, and C. H. Chung.** 2000. Heptameric ring structure of the heat-shock protein ClpB, a protein-activated ATPase in *Escherichia coli*. J. Mol. Biol. **303**:655–666.
15. **Krzewska, J., G. Konopa, and K. Liberek.** 2001. Importance of two ATP-binding sites for oligomerization, ATPase activity and chaperone function of mitochondrial Hsp78 protein. J. Mol. Biol. **314**:901–910.
16. **Lee, G. J.** 1995. Assaying proteins for molecular chaperone activity. Methods Cell Biol. **50**:325–334.
17. **Lee, S., M. E. Sowa, Y. Watanabe, P. B. Sigler, W. Chiu, M. Yoshida, and F. T. F. Tsai.** 2003. The structure of ClpB: a molecular chaperone that rescues proteins from an aggregated state. Cell **115**:229–240.
18. **Lindquist, S., and G. Kim.** 1996. Heat-shock protein 104 expression is sufficient for thermotolerance in yeast. Proc. Natl. Acad. Sci. USA **93**:5301–5306.
19. **Mogk, A., T. Tomoyasu, P. Goloubinoff, S. Rüdiger, D. Röder, H. Langen, and B. Bukau.** 1999. Identification of thermolabile *Escherichia coli* proteins: prevention and reversion of aggregation by DnaK and ClpB. EMBO J. **18**:6934–6949.
20. **Motohashi, K., Y. Watanabe, M. Yohda, and M. Yoshida.** 1999. Heat-inactivated proteins are rescued by the DnaK · J-GrpE set and ClpB chaperones. Proc. Natl. Acad. Sci. USA **96**:7184–7189.
21. **Namy, O., M. Mock, and A. Fouet.** 1999. Co-existence of *clpB* and *clpC* in the Bacillaceae. FEMS Microbiol. Lett. **173**:297–302.
22. **Parsell, D. A., A. S. Kowal, and S. Lindquist.** 1994. *Saccharomyces cerevisiae* Hsp104 protein. Purification and characterization of ATP-induced structural changes. J. Biol. Chem. **269**:4480–4487.
23. **Robert, H., C. L. Marrec, C. Branco, and M. Jebbar.** 2000. Glycine betaine, carnitine, and choline enhance salinity tolerance and prevent the accumulation of sodium to a level inhibiting growth of *Tetragenococcus halophila*. Appl. Environ. Microbiol. **66**:509–517.
24. **Sanchez, Y., and S. Lindquist.** 1990. HSP104 required for induced thermotolerance. Science **248**:1112–1115.
25. **Schirmer, E. C., C. Queitsch, A. S. Kowall, D. A. Parsell, and S. Lindquist.** 1998. The ATPase activity of Hsp104, effects of environmental conditions and mutations. J. Biol. Chem. **273**:15546–15552.

26. **Schlieker, C., I. Tews, B. Bukau, and A. Mogk.** 2004. Solubilization of aggregated proteins by ClpB/DnaK relies on the continuous extraction of unfolded polypeptides. FEBS Lett. **578:**351–356.
27. **Silberg, J. J., K. G. Hoff, and L. E. Vickery.** 1998. The Hsc66-Hsc20 chaperone system in *Escherichia coli*: chaperone activity and interactions with the DnaK-DnaJ-GrpE system. J. Bacteriol. **180:**6617–6624.
28. **Sugimoto, S., J. Nakayama, D. Fukuda, S. Sonezaki, M. Watanabe, A. Tosukhowong, and K. Sonomoto.** 2003. Effect of heterologous expression of molecular chaperone DnaK from *Tetragenococcus halophilus* on salinity adaptation of *Escherichia coli*. J. Biosci. Bioeng. **96:**129–133.
29. **Tosukhowong, A., J. Nakayama, Y. Mizunoe, S. Sugimoto, D. Fukuda, and K. Sonomoto.** 2005. Reconstitution and function of *Tetragenococcus halophila* chaperonin 60 tetradecamer. J. Biosci. Bioeng. **99:**30–37.
30. **Varmanen, P., H. Ingmer, and F. K. Vogensen.** 2000. *ctsR* of *Lactococcus lactis* encodes a negative regulator of *clp* gene expression. Microbiol. **146:** 1447–1455.
31. **Watanabe, Y., K. Motohashi, and M. Yoshida.** 2002. Roles of the two ATP binding sites of ClpB from *Thermus thermophilus*. J. Biol. Chem. **277:**5804–5809.
32. **Weibezahn, J., P. Tessarz, C. Schlieker, R. Zahn, Z. Maglica, S. Lee, H. Zentgraf, E. U. Weber-Ban, D. A. Dougan, F. T. Tsai, A. Mogk, and B. Bukau.** 2004. Thermotolerance requires refolding of aggregated proteins by substrate translocation through the central pore of ClpB. Cell **119:**653–665.
33. **Zolkiewski, M.** 1999. ClpB cooperates with DnaK, DnaJ, and GrpE in suppressing protein aggregation. A novel multi-chaperone system from *Escherichia coli*. J. Biol. Chem. **274:**28083–28086.
34. **Zolkiewski, M., M. Kessel, A. Ginsburg, and M. R. Maurizi.** 1999. Nucleotide-dependent oligomerization of ClpB from *Escherichia coli*. Protein Sci. **8:**1899–1903.

Novel role of neuronal Ca^{2+} sensor-1 as a survival factor up-regulated in injured neurons

Tomoe Y. Nakamura,[1,2] Andreas Jeromin,[4] George Smith,[5] Hideaki Kurushima,[3] Hitoshi Koga,[2] Yusaku Nakabeppu,[3] Shigeo Wakabayashi,[1] and Junichi Nabekura[2,6,7]

[1]Department of Molecular Physiology, National Cardiovascular Center Research Institute, Suita, Osaka 565-8565, Japan
[2]Department of Cellular and System Physiology, Graduate School of Medical Sciences and [3]Division of Neurofunctional Genomics, Department of Immunobiology and Neuroscience, Medical Institute of Bioregulation, Kyushu University, Fukuoka 812-8582, Japan
[4]Neuroscience, Baylor College of Medicine, Houston, TX 77030
[5]Department of Physiology, University of Kentucky Medical School, Lexington, KY 50536
[6]Division of Homeostatic Development, National Institute of Physiological Sciences, Okazaki 444-8585, Japan
[7]Core Research for Evolutional Science and Technology, the Japan Science and Technology Agency, Kawaguchi, Saitama 332-0012, Japan

A molecular basis of survival from neuronal injury is essential for the development of therapeutic strategy to remedy neurodegenerative disorders. In this study, we demonstrate that an EF-hand Ca^{2+}-binding protein neuronal Ca^{2+} sensor-1 (NCS-1), one of the key proteins for various neuronal functions, also acts as an important survival factor. Overexpression of NCS-1 rendered cultured neurons more tolerant to cell death caused by several kinds of stressors, whereas the dominant-negative mutant (E120Q) accelerated it. In addition, NCS-1 proteins increased upon treatment with glial cell line–derived neurotrophic factor (GDNF) and mediated GDNF survival signal in an Akt (but not MAPK)-dependent manner. Furthermore, NCS-1 is significantly up-regulated in response to axotomy-induced injury in the dorsal motor nucleus of the vagus neurons of adult rats in vivo, and adenoviral overexpression of E120Q resulted in a significant loss of surviving neurons, suggesting that NCS-1 is involved in an antiapoptotic mechanism in adult motor neurons. We propose that NCS-1 is a novel survival-promoting factor up-regulated in injured neurons that mediates the GDNF survival signal via the phosphatidylinositol 3-kinase–Akt pathway.

Introduction

Neuronal apoptosis is induced by numerous stressors and underlies many human neurodegenerative disorders, such as Alzheimer's and Parkinson's disease. Under such apoptotic conditions, several neurotrophic factors such as glial cell line–derived neurotrophic factor (GDNF) and brain-derived neurotrophic factor (BDNF) can activate the antiapoptotic process to rescue neurons from death. However, the signaling pathway leading to cell survival is not yet completely understood. GDNF was reported to exert a potent survival-promoting activity in neurons (Henderson et al., 1994; Oppenheim et al., 1995; Yan et al., 1995) and to reduce neuronal death induced by various toxic challenges both in vitro (Nicole et al., 2001) and in vivo (Wang et al., 2002; Kirik et al., 2004). Recent evidence suggests that a part of molecular mechanisms for GDNF-induced cell survival relates to an increase in intracellular Ca^{2+} concentration, and it subsequently activates some survival pathways such as the phosphatidylinositol 3-kinase (PI3-K)–Akt pathway (Perez-Garcia et al., 2004).

Ca^{2+} is the most versatile and important intracellular messenger in neurons, regulating a variety of neuronal processes such as neurotransmission and signal transductions. The various actions of Ca^{2+} are mediated by a large family of EF-hand Ca^{2+}-binding proteins, which may act as Ca^{2+} sensors or Ca^{2+} buffers. One of them, neuronal Ca^{2+} sensor-1 (NCS-1; mammalian homologue of frequenin), was originally identified in *Drosophila melanogaster* in a screen for neuronal hyperexcitability mutants (Mallart et al., 1991). Overexpression of NCS-1 has been shown to enhance evoked neurotransmitter release and exocytosis (Pongs et al., 1993; Olafsson et al., 1995). NCS-1 directly interacts with phosphatidylinositol 4-hydroxykinase (PI4-K; Hendricks et al., 1999; Weisz et al., 2000) and enhances neuronal secretion by modulating vesicular trafficking steps in

Correspondence to Tomoe Y. Nakamura: tomoen@ri.ncvc.go.jp

Abbreviations used in this paper: BDNF, brain-derived neurotrophic factor; DMV, dorsal motor nucleus of the vagus; GAPDH, glyceraldehyde-3-phosphate dehydrogenase; GDNF, glial cell line–derived neurotrophic factor; MEK, MAPK kinase; NCS-1, neuronal Ca^{2+} sensor-1; PH, pleckstrin homology; PI3-K, phosphatidylinositol 3-kinase; PI4-K, phosphatidylinositol 4-hydroxykinase.

The Journal of Cell Biology, Vol. 172, No. 7, March 27, 2006 1081–1091
http://www.jcb.org/cgi/doi/10.1083/jcb.200508156

a phosphoinositide-dependent manner (Koizumi et al., 2002). We have previously demonstrated that NCS-1 modulates the voltage-gated K^+ channel Kv4 (Nakamura et al., 2001). Subsequently, certain voltage-gated Ca^{2+} channels have also been reported to be regulated by NCS-1 (Weiss et al., 2000; Wang et al., 2001; Tsujimoto et al., 2002). Furthermore, NCS-1 enhances the number of functional synapses (Chen et al., 2001), potentiates paired pulse facilitation (Sippy et al., 2003), and may be involved in associative learning and memory in *Caenorhabditis elegans* (Gomez et al., 2001). Despite the participation of NCS-1 in a wide range of biological functions, however, the role of NCS-1 in neuronal survival under pathophysiological conditions or the involvement of NCS-1 in neurotrophic factor–mediated neuroprotection are unknown.

Because we found that the expression levels of NCS-1 is significantly higher in immature brain (Nakamura et al., 2003) and a remarkable similarity exists between immature and injured neurons during the development and regeneration process, respectively (Nabekura et al., 2002b), these findings prompted us to study the expression level and the functional roles of NCS-1 in damaged neurons.

In this study, we found that NCS-1 is a survival-promoting factor, which increases the resistance of neurons to several kinds of stressors. In addition, NCS-1 is up-regulated in response to axonal injury in adult motor neurons, and this protects cells from apoptosis. Furthermore, NCS-1 mediates GDNF-induced neuroprotection via activation of Akt pathways. This is the first study demonstrating a novel role of NCS-1 on neuronal survival.

Results

The expression level of NCS-1 protein increases with neuronal injury

To examine the expression level of NCS-1 in injured neurons, we performed unilateral vagal axotomy (transaction of nerves) on adult rats. 1 d to 2 mo after the in vivo axotomy, brainstems, including the bilateral dorsal motor nucleus of the vagus (DMV) neurons, were isolated. Immunohistochemical staining and computerized image analysis of frozen sections revealed that axotomy significantly (more than threefold) increased the expression level of NCS-1 in the DMV when compared with those on the control side at 1 wk after the surgery (Fig. 1, A–C). NCS-1 immunoreactivity was mainly expressed in cell bodies of neurons, as shown using hematoxylin counterstaining to identify the nuclei (Fig. 1 B, brown staining accompanied with blue staining; depicted by arrows). The increase in NCS-1 level started at 1 d after axotomy, reached a peak at 1 wk, and gradually decreased to control levels over the next 2 mo (Fig. 1 D). We also conducted quantitative immunoblot analysis on tissue samples from DMV neurons 1 d and 1 wk after axotomy, expressing NCS-1 density relative to levels of glyceraldehyde-3-phosphate dehydrogenase (GAPDH). The results confirmed the immunohistochemistry experiments, with levels of NCS-1 protein in ipsilateral DMV being increased significantly (by about threefold) by 1 wk after axotomy (Fig. 1, E and F).

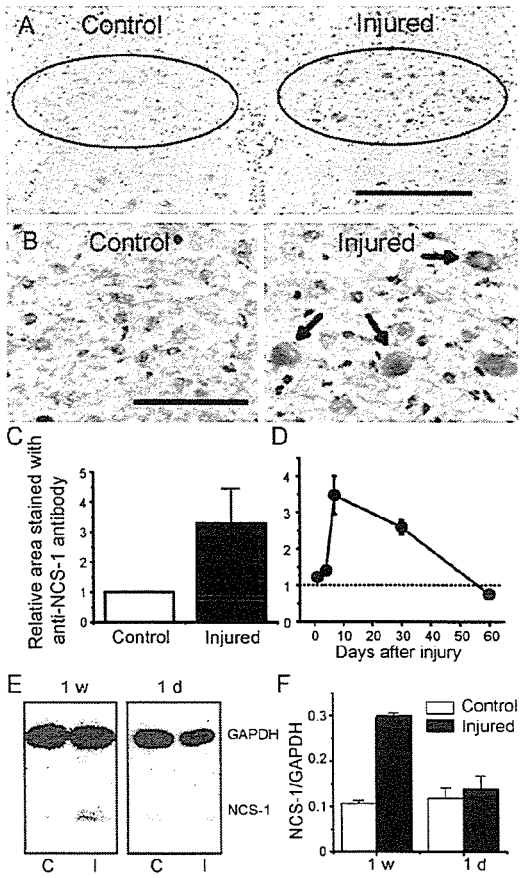

Figure 1. **NCS-1 is up-regulated in the DMV neurons after in vivo axotomy.** The 10th cranial nerve on one side of the neck of adult (4–6-wk-old) rats was cut, and, 1 d to 2 mo later, the brainstem was excised and frozen sections were cut. The NCS-1 expression was examined by counterstaining with NCS-1 antibody (brown signal) and with hematoxylin to identify nuclei (blue signal). (A) Staining pattern 1 wk after in vivo axotomy. The amount of NCS-1 protein increased in the DMV neurons ipsilateral to axotomy (injured side) when compared with control neurons contralateral to axotomy. Positions of DMV neurons are represented by circles. (B) Magnified image of DMV neurons. Arrows indicate that some neurons have both NCS-1 and hematoxylin staining, indicating that NCS-1 is expressed in cell bodies. Bars (A), 200 μm; (B) 50 μm. (C) Summarized data obtained by computerized image analysis. The relative area stained using NCS-1 antibody on the injured side 1 wk after axotomy was normalized to that of the control side (means ± SEM [error bars]; $n = 6$). (D) Time course of the expression levels of NCS-1 in injured DMV neurons relative to uninjured DMV neurons. Immunohistochemical analysis of NCS-1 levels were performed in rats 1, 4, 7, 30, and 60 d after axotomy (means ± SEM; $n = 6$). (E) Immunoblots indicating the expression levels of NCS-1 in the tissue samples obtained from DMV regions in brainstem sections at control (C) and injured sites (I) 1 wk and 1 d after axotomy. 10 sections were used for each group. Similar amount of proteins were loaded on the gel as indicated by the similar amount of the internal control GAPDH. (F) The densities of NCS-1 bands were expressed relative to the density of GAPDH bands in each tissue sample, and the group data is summarized (means ± SEM; $n = 3$).

Up-regulation of NCS-1 protein was also observed using a different type of stressor. Continuous treatment of neurons with colchicine for 4 d, which disrupts tubulin polymerization and blocks axonal transport, also increased NCS-1 expression levels (1.40 ± 0.03-fold above control levels; $P < 0.05$; $n = 4$), indicating that NCS-1 is up-regulated in vivo in response to two

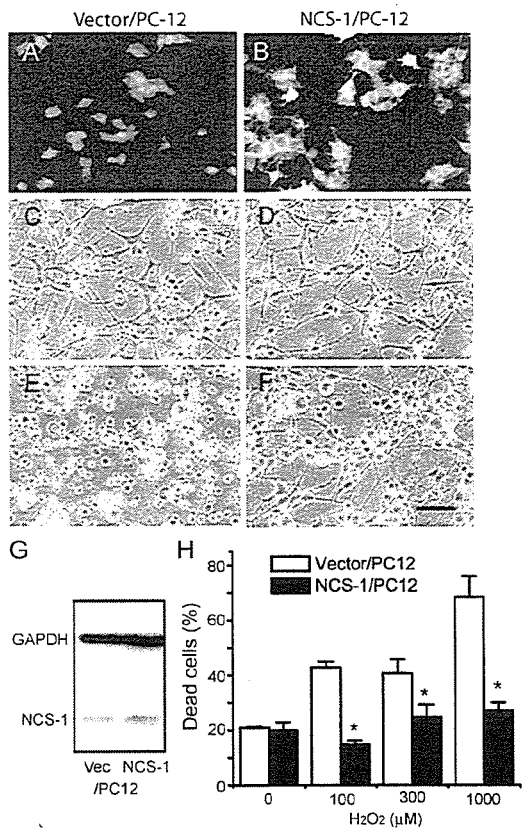

Figure 2. **Effects of the overexpression of NCS-1 on the susceptibility of PC-12 cells to H_2O_2 toxicity.** PC-12 cells stably transfected with NCS-1 (NCS-1/PC12) or vector alone (vector/PC-12) were differentiated into neuronlike cells by treatment with 100 ng/ml NGF and exposed to several concentrations (0–1 mM) of H_2O_2. (A and B) Immunofluorescent micrographs show that the expression level of NCS-1/PC12 cells is much higher than that in vector/PC12 cells. (C–F) Phase-contrast micrographs of PC-12 cells exposed to 0 (C and D) or 300 μM H_2O_2 for 3 d (E and F). Bar, 40 μm. (G) Representative immunoblots showing expression levels of NCS-1 in control vector and NCS-1–transfected cells. Also shown is the expression levels of the control protein GADPH obtained from immunoblots from the same cell samples. Unlike for NCS-1 levels, GADPH levels were not markedly different in control and NCS-1–transfected cells. (H) Bar graph shows the cell viability evaluated by trypan blue exclusion assay (means ± SEM [error bars]; $n = 8$). *, $P < 0.05$ versus vector/PC-12 cells.

different kinds of stressors—one being mechanical and the other being chemical injury.

Expression of NCS-1 renders PC-12 cells more tolerant to stressors

To study the physiological role of NCS-1 in damaged neurons, we next examined the effect of NCS-1 overexpression on the susceptibility of cells to several kinds of stressors. PC-12 cells stably transfected with either the NCS-1 expression vector (NCS-1/PC-12) or the vector alone (vector/PC-12) were differentiated into neuronlike cells, and the resistance to H_2O_2 toxicity was compared between these two groups. As shown in the immunofluorescent micrographs and immunoblot in Fig. 2 (A, B, and G), the expression level of NCS-1 was found to be significantly higher in NCS-1/PC-12 cells compared with vector-transfected cells, although these cells also had some endogenous NCS-1. Treatment with a relatively high dose (300 μM) of H_2O_2 for 3 d in the absence of pyruvate resulted in severe cellular damage in vector/PC-12 control cells; most cells were rounded up and detached from the substratum (Fig. 2 E). In contrast, the same treatment caused only a little damage to cells overexpressing NCS-1 (Fig. 2 F), indicating that the expression of NCS-1 rendered PC-12 cells more tolerant to H_2O_2 toxicity. The expression of NCS-1 reduced cell death caused by treatment with up to 1,000 μM H_2O_2 (Fig. 2 H). The aforementioned results were obtained from three cell lines transfected with NCS-1 and with corresponding vector-transfected control. A similar beneficial effect of NCS-1 on cell survival in response to 300 μM H_2O_2 was seen in two PC-12 cell lines that were not treated with NGF (not depicted).

NCS-1 promotes the long-term survival of primary cultured cortical neurons under stress and normal conditions

To further confirm the involvement of NCS-1 in neuronal survival, we overexpressed NCS-1 or its mutant E120Q in primary cultured embryonic rat cortical neurons that express endogenous NCS-1. The E120Q mutant possesses an amino acid substitution within the third EF-hand Ca^{2+}-binding motif, which impairs Ca^{2+} binding (Jeromin et al., 2004) but preserves the interaction with target proteins and, thereby, exerts a dominant-negative effect by disrupting the function of endogenous NCS-1 (Weiss et al., 2000). We used an adenoviral transfer system to transiently deliver the cDNA encoding NCS-1 together with EGFP (using an internal ribosome entry site–containing vector) and its E120Q mutant form into neurons cultured for 5 d in neurobasal medium containing B27 trophic supplements. As indicated by cells with EGFP fluorescence and nuclei stained with Hoechst 33258, nearly 70% of neurons were successfully infected with each virus at 3 d after infection (Fig. 3 A). We examined the effects of overexpression of wild-type and dominant-negative NCS-1 on neuronal survival under stress caused by B27 withdrawal, which has been reported to induce neuronal apoptosis (Brewer, 1995; Cheng et al., 2003). As shown in Fig. 3 B, B27 withdrawal promoted cell death in vector-treated control neurons (left; also compare the vector groups with and without B27 in Fig. 3 D). Overexpression of NCS-1, on the other hand, significantly rescued cells from death (Fig. 3 B, middle). In contrast, the expression of E120Q resulted in more severe cell death accompanying bleb formation (Fig. 3 B, right). To quantitatively analyze the time course for the changes in cell viability, the total number of surviving cells from the same field was counted daily by phase-contrast microscopy during 9 d (see Materials and methods). The results show that high cell viability was preserved upon expression of the wild-type NCS-1, whereas cell viability was reduced after the expression of E120Q; i.e., the number of days required to reach 70% cell viability were 5, 8, and 3 d for vector, NCS-1, and E120Q groups, respectively (Fig. 3 C). The expression levels of NCS-1 in each group of neurons before and after adenovirus infection in the absence of B27 trophic supplements are shown in the immunoblot (Fig. 3 E). Essentially the same results were obtained by counting neurons with condensed nuclei using

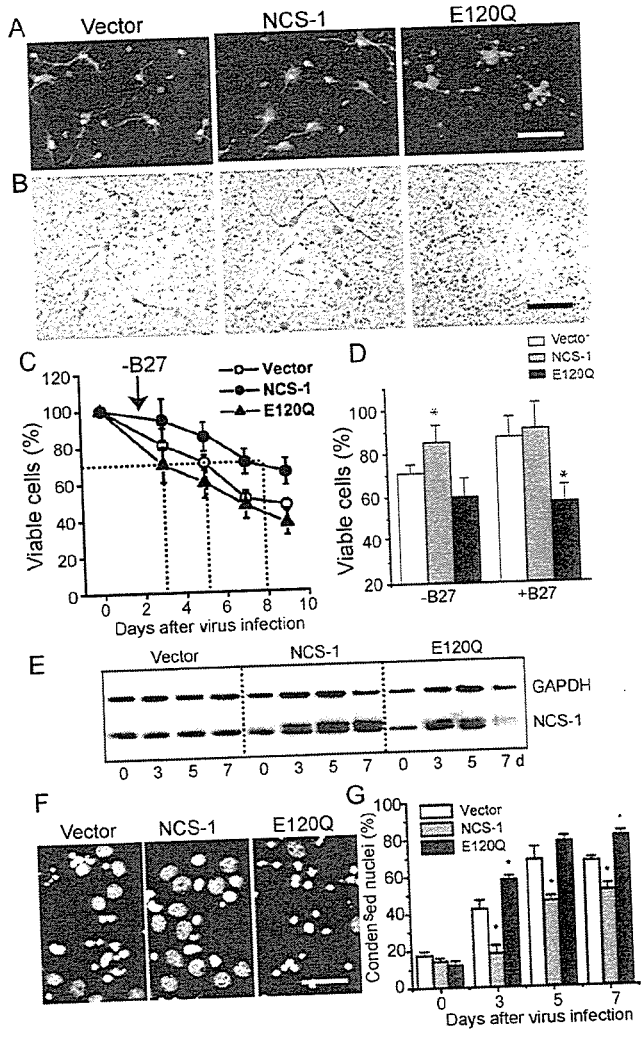

Figure 3. **Survival-promoting effect of NCS-1 in primary cultured cortical neurons.** Neurons were infected with adenovirus carrying EGFP vector alone, NCS-1, and its EF-hand mutant (E120Q) together with EGFP in the same internal ribosome entry site vector in culture medium containing neurobasal medium plus B27 trophic supplements, and they were further cultured in the presence or absence of B27 supplements (B27 supplements were withdrawn 2 d after the virus infections). (A) Fluorescent micrographs show the cultured neurons treated with adenovirus for 3 d (exhibiting strong EGFP signals) followed by treatment with a DNA-binding dye Hoechst 33258 to label their nuclei (red signals, pseudo-colored). (B) Phase-contrast micrographs show the cultured neurons treated with adenovirus for 5 d in the absence of B27 trophic supplements. Bars, 40 μm. (C) Time course of cell viability for neurons infected with adenovirus in the absence of B27 trophic supplements. Living neurons were counted daily by phase-contrast microscopy and plotted as a percentage of the initial number of neurons present on day 0 (n = 4). The number of days required to reach 70% cell viability is shown by the dotted lines. (D) Summary of cell viability data obtained from neurons cultured in the absence and presence of B27 trophic supplements at 5 d after virus infection. Error bars represent SEM. *, $P < 0.05$ versus the vector-controlled group. (E) Expression levels of NCS-1 and GAPDH in cultured neurons infected with each adenovirus indicated in the absence of B27 trophic supplements. (F and G) Staining patterns (light blue and white signals) of nuclei with Hoechst 33258 (F) and normalized numbers of cells having condensed nuclei (G). The dark blue color was changed to light blue or white to visualize signals more clearly. Bar, 15 μm.

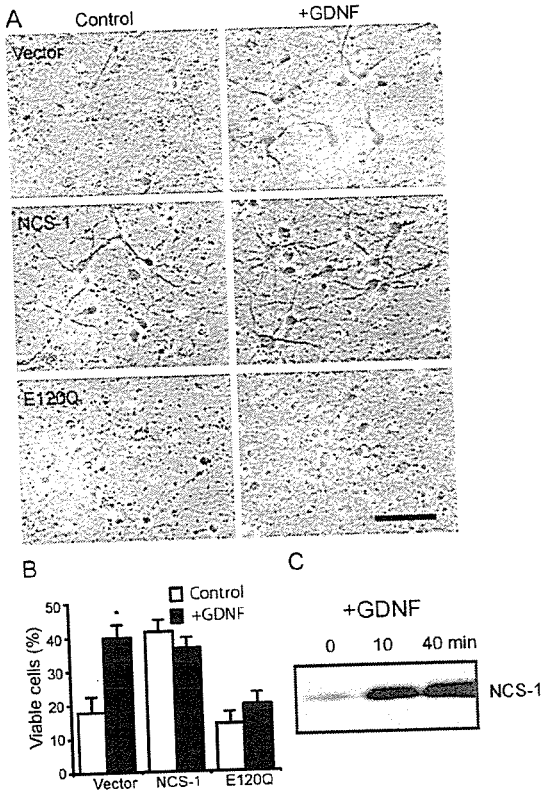

Figure 4. **NCS-1 mediates GDNF-induced neuronal survival.** (A) Primary cultured cortical neurons infected with adenovirus carrying vector alone (top), NCS-1 (middle), or E120Q mutant (bottom) were treated for 2 d with or without 10 ng/ml GDNF under the condition where B27 trophic supplement was depleted. Bar, 40 μm. (B) Summary of cell viability data. Viable cells were counted 2 d after GDNF treatment (+GDNF) or no treatment (control) and plotted as the percentage of the initial number of neurons present at day 0 in the same visual field (mean ± SEM [error bars]; n = 4). All neurons, not just transfected cells, were included in the cell viability counts. Note that treatment with E120Q largely prevented the GDNF-induced neuronal survival effect. *, $P < 0.05$ versus the data without exposure to GDNF. (C) Expression levels of NCS-1 in cultured neurons treated with 10 ng/ml GNDF for the indicated times.

Hoechst staining (Fig. 3, F and G), thus reinforcing the finding that the expression of NCS-1 protects neurons from cell death under apoptotic conditions. Furthermore, when B27 trophic supplement was kept in the culture medium (which is a less stress condition), the dominant-negative effect of E120Q was more clearly observed when compared with the vector control group (Fig. 3 D; also see A, where some blebs were observed in the neurons infected with E120Q mutant). In other preliminary experiments (not depicted), although the time course of the loss in cell viability was variable, overexpression of NCS-1 consistently delayed the loss of cell viability when B27 supplements were omitted, and the expression of E120Q always increased the rate of cell death when B27 was present. These results suggest that endogenous NCS-1 is playing an important role in keeping the long-term survival of cultured neurons under normal conditions in addition to the protective role from stress under apoptotic conditions.

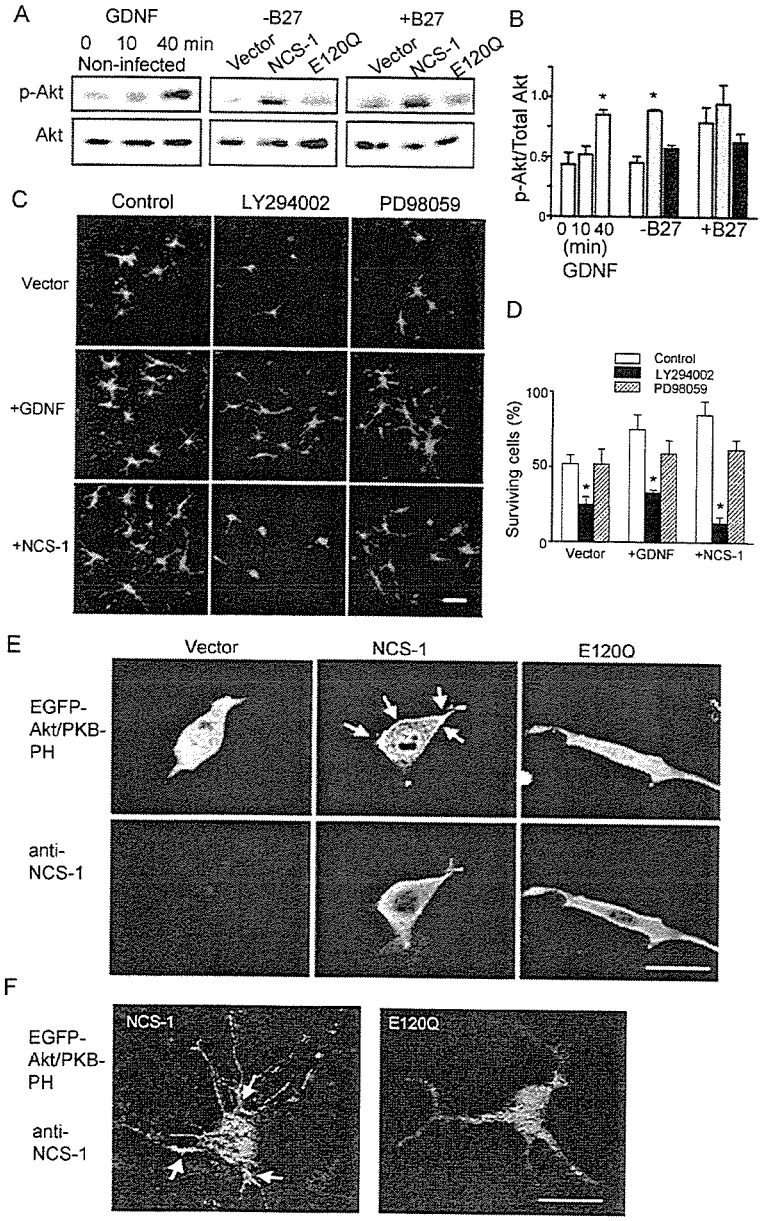

Figure 5. **NCS-1 promotes neuronal survival via activation of the PI3-K–Akt pathway.** (A and B) Both NCS-1 expression and GDNF treatment increase the phosphorylation of Akt kinase. Primary cultured cortical neurons were treated with 10 ng/ml GDNF for the indicated time periods or were infected with adenovirus carrying vector, NCS-1, or E120Q mutant and further incubated for 7 d in the presence or absence of B27 trophic supplements. They were then subjected to immunoblot analysis to detect protein levels of total (Akt) and phosphorylated form (p-Akt, the mixture of anti–P-Ser-473 and anti–P-Thr-308 antibodies, was used; A). The densities of phosphorylated Akt were normalized by those of total Akt levels and summarized in the bar graph (B). *, $P < 0.05$ versus vector control. (C and D) Both GDNF- and NCS-1–induced neuronal survival were abolished by PI3-K inhibitor but not by MEK inhibitor. Primary cultured cortical neurons were infected with adenovirus carrying NCS-1 or vector alone in medium lacking B27 trophic supplements. 3 d later, cultures were treated with 20 μM LY294002 or PD98059. For the vector-treated group, some cultures were further treated with 10 ng/ml GDNF. (C) Adenovirus-infected viable neurons treated or untreated with GDNF for 3 d. Bar, 40 μm. (D) Viable cells were counted and plotted as the percentage of the initial number of neurons present on day 0 (means ± SEM [error bars]; $n = 4$). *, $P < 0.05$ versus the data with no inhibitors. (E and F) NCS-1 activates Akt kinase by increasing the plasma membrane $PtdIns(3,4)P_2$ and $PtdIns(3,4,5)P_3$ levels in both CCL39 cells (E) and cultured neurons (F). CCL39 cells and primary cultured rat cortical neurons were transiently transfected with EGFP-Akt/PKB-PH together with either pCDNA3, NCS-1, or E120Q (1:3 ratios). 2 d later, cells were fixed, and immunocytochemistry was performed to detect NCS-1 proteins. Both EGFP distribution (E, top; and F, green signals) and NCS-1 expression (E, bottom; and F, red signals) were visualized using a laser confocal microscope. Laser confocal sections through the middle of representative cells in each treatment are shown. Arrows indicate the peripheral redistribution of the EGFP–PKB–PH in NCS-1–expressing cells. Bars, 10 μm.

NCS-1 mediates GDNF-induced cell survival

A large body of evidence suggests that neuronal survival is promoted by neurotrophic factors such as BDNF and GDNF (Boyd and Gordon, 2003). Because the long-term application of GDNF has been reported to enhance the expression of NCS-1 in *Xenopus laevis* motor neurons (Wang et al., 2001), we attempted to clarify the role of NCS-1 as a downstream mechanism of GDNF-induced cell survival in rat cortical neurons. When primary cultured cortical neurons were treated with 10 ng/ml GDNF for 2 d after the withdrawal of B27 supplements, neuronal survival was significantly enhanced when compared with time-matched control (Fig. 4, A [top] and B). Interestingly, the expression of NCS-1 mimicked the survival-promoting effects of GDNF; i.e., NCS-1 exerted a robust survival effect even in the absence of GDNF (Fig. 4, A [middle] and B). Most strikingly, the expression of the dominant-negative NCS-1 mutant E120Q largely prevented cell survival induced by GDNF (Fig. 4, A [bottom] and B). Immunoblot analysis revealed that the application of 10 ng/ml GDNF resulted in a significant increase in the expression level of endogenous NCS-1 within 10 min, which further increased at 40 min in these neurons (Fig. 4 C). The amount of NCS-1 remained elevated through 2 d of exposure to GDNF (not depicted). These results show that the treatment of GDNF increases the expression level of NCS-1, which subsequently promotes neuronal survival, suggesting that GDNF-induced neuroprotection is at least in part mediated by NCS-1.

Activation of the PI3-K–Akt pathway is involved in NCS-1–induced neuronal survival

In neurons, GDNF has been reported to promote cell survival via activation of signaling cascades involving the PI3-K–Akt pathway (Soler et al., 1999; Takahashi, 2001). In accordance with these studies, we also observed that exposure of primary cultured cortical neurons to GDNF resulted in a large increase in phospho-Akt levels (Fig. 5 A, left). Therefore, it was of interest for us to test whether NCS-1 also activates this kinase. We examined the effect of NCS-1 expression or its dominant-negative form on Akt phosphorylation in the presence or absence of B27 trophic supplements. When B27 trophic supplements were absent, the expression of NCS-1 significantly enhanced the phosphorylation of Akt, whereas expression of the dominant-negative mutant E120Q had little effect when compared with control vector-infected neurons (Fig. 5, A [middle] and B). On the other hand, when B27 supplements were present, a relatively high level of phosphorylated Akt was observed in the vector-treated control group (Fig. 5, A [right] and B). Additional expression of exogenous NCS-1 further increased the Akt phosphorylation level, whereas expression of the dominant-negative mutant suppressed phosphorylation (Fig. 5, A [right] and B). Thus, the phosphorylation levels of Akt in each group of neurons were well correlated with their viabilities, as shown in Fig. 3 D.

In addition, pretreatment of cultured cortical neurons with LY294002, an inhibitor of PI3-K, completely abolished both GDNF- and NCS-1–induced neuronal survival, whereas PD98059, an inhibitor of MAPK kinase (MEK), did not (Fig. 5, C and D). These results suggest that the NCS-1–induced survival-promoting effect is mediated via the PI3-K–Akt pathway but not the MAPK pathway in cultured cortical neurons.

To further understand the upstream mechanism of the NCS-1–induced activation of Akt, we next examined the effect of overexpression of NCS-1 and E120Q on the subcellular localization of Akt/PKB in living cells. Akt/PKB is known to be translocated to the plasma membrane when it is fully activated upon phosphorylation and bound with its substrates PtdIns(3,4)P_2 and PtdIns(3,4,5)P_3 (Alessi et al., 1996). We constructed the GFP-tagged pleckstrin homology (PH) domain of Akt/PKBα (EGFP-Akt/PKB-PH) and transiently cotransfected it into CCL39 cells, which express a small amount of endogenous NCS-1, together with NCS-1, E120Q, or empty vector. 2 d later, the subcellular localization of EGFP-tagged Akt/PKB-PH was assessed on a confocal microscope. Akt/PKB-PH was diffusely localized in the cytosol of vector-transfected control cells (Fig. 5 E). Interestingly, Akt/PKB-PH became localized in the peripheral region of cells when NCS-1 was coexpressed, but this peripheral localization was abolished when E120Q was coexpressed (Fig. 5 E). Qualitatively similar results were also obtained when primary cultured cortical neurons were treated with the same vectors; i.e., Akt/PKB-PH was localized in the peripheral regions of neurons when NCS-1 was overexpressed, but a more diffuse localization pattern was observed when E120Q was overexpressed (Fig. 5 F). The distribution pattern of Akt/PKB-PH in vector-transfected neurons was similar to that of NCS-1–overexpressing cells (not depicted). These results strongly demonstrate that NCS-1 increases the levels of plasma membrane PtdIns(3,4)P_2 and PtdIns(3,4,5)P_3 and, thus, activates Akt/PKB in living cells.

Dominant-negative NCS-1 accelerates the in vivo axotomy-induced loss of neurons

We examined the effects of the overexpression of NCS-1 and its dominant-negative mutant on the survival of these neurons to clarify the physiological role of NCS-1 in injured motor neurons in vivo. One side of vagus nerves of adult rats were axotomized as previously described (Fig. 1) and infected with adenoviral vectors encoding NCS-1, E120Q, or EGFP vector alone, and neuronal degeneration was evaluated by histological analysis. 1 wk after axotomy, nearly 30% of nerve cells were found to be EGFP positive in the injured side (Fig. 6 A). There were clear differences in the staining pattern between control and injured sides for all groups, probably because the regeneration process, such as activation of the surrounding glial cells, was ongoing on injured sides. However, the number of surviving motor neurons stained with hematoxylin were not significantly decreased at the injured side for vector-treated DMV sections (Fig. 6, B and D; examples of counted neurons are indicated by black arrows in C). This would probably be the result of natural antiapoptotic mechanisms induced by injury, which exist in mature neurons as previously reported (Benn and Woolf, 2004). Because the expression level of NCS-1 was significantly increased in response to in vivo axotomy (Fig. 1), we hypothesized that NCS-1 may be involved in this antiapoptotic mechanism. If so, blocking of endogenous NCS-1 would reduce this beneficial effect. As expected, the dominant-negative E120Q mutant resulted in a significant loss of neurons in the injured side (Fig. 6, B–D), and some TUNEL-positive nuclei were also detected only in this group (Fig. 6 E, arrows; and its magnified image in F). Considering that the infection efficiency was only ~30% in these experiments, a large majority of neurons successfully infected with E120Q appear to have undergone apoptosis. Infection of neurons with the functional NCS-1 adenovirus only had a modest effect on neuronal survival. This probably results from both the low infection efficiency and the high levels of endogenous NCS-1 expression in axotomized neurons (Fig. 1) because the NCS-1 effects are already close to maximum. Thus, the dominant-negative mutant E120Q inhibited the survival of adult DMV neurons from axotomy-induced injury, strongly suggesting that NCS-1 is one of the important factors mediating neuronal survival after in vivo axotomy.

Discussion

Numerous stressors, including physical or chemical injury and genetic abnormalities, lead to neuronal degeneration by programmed cell death along an apoptotic pathway. Under these conditions, some intrinsic and extrinsic factors, including neurotrophic factors, are known to activate the antiapoptotic process to rescue neurons from death. However, the signaling pathway leading to cell survival is not yet completely understood.

In this study, we identified a novel function for the Ca^{2+}-binding protein NCS-1, which (1) promotes the long-term survival

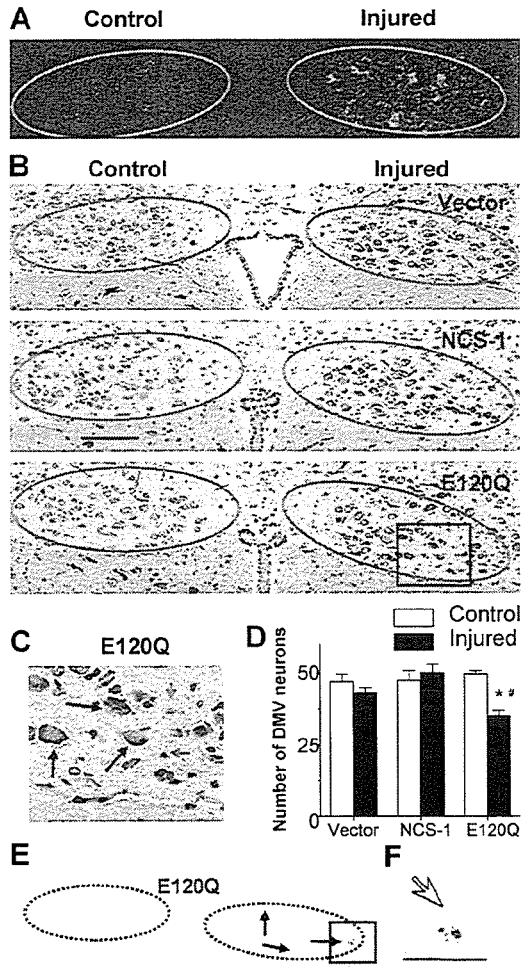

Figure 6. **Dominant-negative NCS-1 mutant E120Q promotes the axotomy-induced degeneration of DMV neurons.** After the axotomy of vagus motor neurons were performed as described in Fig.1, adenoviral vectors carrying NCS-1, E120Q, or EGFP alone were injected from the stump of the nerve. 1 wk after the treatment, the brainstem was excised, and serial sections were cut. (A) Representative EGFP fluorescence image showing that EGFP signals were detected in some cells on the injured side. Positions of DMV neurons are indicated by circles in A, B, and E. (B) Histological evaluation of DMV neurons in adenovirus-treated animals by hematoxylin/eosin staining. (C) Magnified image of the boxed area in B for E120Q-treated DMV neurons. Only neurons (indicated by black arrows), not nuclei, of glial or endothelial cells (indicated by red arrows) were counted. (D) Summarized data obtained from B. *, $P < 0.05$ versus the control side of the same section. #, $P < 0.05$ versus the injured side of vector-treated animals (means ± SEM [error bars]; $n = 6$ from three animals). (E) An example of the TUNEL-staining pattern obtained from an E120Q-treated animal. (F) The magnified image of the boxed area in E. TUNEL-positive nuclei are indicated by arrows. Bar (B), 100 μm; (F) 25 μm.

of cultured neurons via PI3-K–Akt signaling pathways; (2) mediates, at least in part, GDNF-induced neuroprotection; and (3) is up-regulated in response to axonal injury and plays an important role in the antiapoptotic mechanism in injured motor neurons.

NCS-1 is a novel survival-promoting factor in neuronal cells

We observed that the overexpression of NCS-1 rendered PC-12 cells and primary cultured cortical neurons more tolerant to several kinds of stressors, such as oxidative stress or trophic supplement withdrawal (Figs. 2 and 3), demonstrating that the expression of NCS-1 protects neurons from cell death under apoptotic conditions. In addition, overexpression of an EF-hand dominant-negative mutant E120Q significantly accelerated apoptosis when B27 trophic supplements were kept in the culture medium (Fig. 3 D), suggesting that endogenous NCS-1 is important for keeping the long-term survival of cultured neurons under normal (or less apoptotic) conditions. The latter finding also indicates that Ca^{2+} binding is required for NCS-1–mediated cell survival. On the basis of these findings, we propose that NCS-1 is a novel member of survival-promoting factors in cultured neurons.

NCS-1 mediates GDNF-induced cell survival via activation of the PI3-K–Akt survival pathway

We found that treatment of cultured cortical neurons with a neurotrophic factor GDNF increased the expression level of NCS-1 (Fig. 4 C) and enhanced neuronal survival (Fig. 4, A and B), which is consistent with a previous study reporting that GDNF enhanced the expression of frequenin/NCS-1 in *Xenopus* motor neurons (Wang et al., 2001). GDNF-induced increase in the NCS-1 level appeared to be caused by the synthesis of protein and/or mRNA but not by the prevention of NCS-1 degradation because GDNF did not raise the expression level of NCS-1 in the presence of the inhibitor of protein synthesis cycloheximide (10 μg/ml for 20 h; not depicted). In contrast to the vector-treated control neurons, GDNF did not further enhance the survival effect in neurons overexpressing NCS-1 (Fig. 4, A and B), suggesting that cell viability was already sufficiently high under this condition. Strikingly, the survival-promoting effect of GDNF was largely prevented by overexpression of the dominant-negative mutant E120Q (Fig. 4, A and B), suggesting that NCS-1 mediates the GDNF survival signal.

GDNF activates at least two intracellular pathways in neurons: one involving the PI3-K–Akt pathway and another involving the MAPK (p42 and p44, also called ERK1 and ERK2) pathway. However, PI3-K but not the MAPK pathway has been reported to be responsible for GDNF-mediated neuronal survival in motor neurons (Soler et al., 1999). In accordance with this study, we observed that exposure of primary cultured cortical neurons to GDNF resulted in a large increase in the phospho-Akt level (Fig. 5 A). In the same way, the overexpression of NCS-1 also dramatically enhanced the phosphorylation levels of Akt both in the presence and absence of B27 trophic supplements, whereas the overexpression of dominant-negative mutant E120Q did not (Fig. 5 A). In addition, the NCS-1–nduced survival-promoting effect was largely inhibited by the PI3-K inhibitor LY294002 but not the MEK inhibitor PD98059 (Fig. 5, C and D). Furthermore, NCS-1 increased the plasma membrane $PtdIns(3,4)P_2$ and $PtdIns(3,4,5)P_3$ levels, which indicates the activation of Akt in intact cells (Fig. 5, E and F). These results strongly suggest that NCS-1 is a novel downstream target that mediates GDNF survival signal through activation of the PI3-K–Akt pathway.

Possible mechanisms of the action of NCS-1

Several possible mechanisms may underlie the survival action of NCS-1. We observed that Akt/PKB-PH was recruited to the plasma membrane when NCS-1 was coexpressed, suggesting that NCS-1 acts upstream of the Akt pathway. NCS-1 was previously reported to activate PI4-K (Hendricks et al., 1999), which increases the level of plasma membrane PtdIns(4)P, the substrate of PI3-K, as well as PI5-K. Therefore, upon activation of these kinases, other phosphoinositides would be produced. Indeed, it has been reported that the overexpression of NCS-1 significantly increased both PtdIns(4)P and PtdIns(4,5)P_2 levels in PC-12 cells (Koizumi et al., 2002). Furthermore, PtdIns(3,4)P_2 and PtdIns(3,4,5)P_3, the substrates of Akt/PKB, would also be produced, which, in turn, would activate the Akt pathway (Cantley, 2002). As expected, the overexpression of NCS-1 increased the plasma membrane PtdIns(3,4)P_2 and PtdIns(3,4,5)P_3 levels both in CCL39 cells and neuronal cells (Fig. 5, E and F), enhanced the phosphorylation of Akt (Fig. 5 A), and promoted neuronal survival (Fig. 3). Therefore, we propose that activation of such a phosphatidylinositol pathway is a mechanism for the survival action of NCS-1. In addition, we observed that in contrast to GDNF, our preliminary data show that BDNF did not increase the expression level of NCS-1 (unpublished data) despite the reported survival-promoting effect of BDNF in cultured cortical neurons (Cheng et al., 2003). Interestingly, BDNF-induced survival signaling has been reported to be mediated by CaM, another Ca^{2+}-binding protein in cortical neurons (Cheng et al., 2003), and CaM has been reported to directly activate PI3-K (Perez-Garcia et al., 2004). Therefore, NCS-1 mediates the GDNF signal by activating PI4-K, whereas CaM mediates the BDNF signal by activating PI3-K. These two signals would lead the survival signal to the Akt pathway.

On the other hand, it is also possible that NCS-1 promotes neuronal survival by some other mechanisms in addition to activation of the Akt pathway. For example, the survival-promoting effect of NCS-1 appears to be analogous to that of the recently characterized antiapoptotic protein family called inhibitors of apoptosis, which suppress apoptosis through the direct inhibition of caspases (Liston et al., 2003). Some of these proteins, such as neuronal apoptosis inhibitory protein and X-linked inhibitors of apoptosis protein, have been reported to be essential for GDNF-mediated neuroprotective effects in injured motor neurons in vivo (Perrelet et al., 2002). Furthermore, recent evidence demonstrates that neuronal apoptosis inhibitory protein interacts with hippocalcin, another closely related Ca^{2+}-binding protein that affects caspase-12 activity (Korhonen et al., 2005) and protects neurons against Ca^{2+}-induced cell death (Mercer et al., 2000). Therefore, we do not exclude the possibility that like these proteins, NCS-1 also exerts a more direct effect on some caspases. We are currently investigating the possible interaction of these proteins.

As NCS-1 is known to interact with voltage-gated K^+ channels (Kv4; Nakamura et al., 2001), it might also increase the resistance of neurons to excitotoxic apoptosis through the activation of K^+ channels. Increased outward K^+ current would prevent neurons from reaching firing threshold and, thereby, prevent cells from Ca^{2+} overload leading to cell death.

NCS-1 is a novel survival-promoting factor up-regulated in injured neurons

In this study, we found that the expression level of NCS-1 was significantly increased in response to axonal injuries (transection of the vagus nerve as well as treatment of nerves with colchicine) in the DMV neurons of adult rats (Fig. 1). The behavior of NCS-1 appears to be analogous to that of the recently identified protein damage-induced neuronal endopeptidase, which is expressed in response to neuronal damages induced by nerve transection and colchicine treatment in both the central and peripheral nervous systems (Kiryu-Seo et al., 2000). Because antiapoptotic mechanisms are activated in mature neurons in response to stress to protect against accidental apoptotic cell death, it has been described that peripheral axotomy in adult neurons does not result in extensive cell death (Benn and Woolf, 2004). In accordance with this, we also observed that little loss of motor neurons was evident by in vivo axotomy in vector-treated control neurons (Fig. 6, B and D). The expression of exogenous NCS-1 did not exert the further beneficial effect (Fig. 6, B and D). This marginal effect of exogenous NCS-1 (compared with the vector control group) would be the result of the increased expression level of endogenous NCS-1 in axotomized neurons, which occurs for all groups. In contrast, overexpression of dominant-negative E120Q significantly decreased the number of surviving neurons (Fig. 6, B–D) and produced TUNEL-positive apoptotic neurons at the injured side (Fig. 6, E and F), indicating that disruption of NCS-1 function increased the vulnerability of DMV neurons to axotomy.

Overexpression of NCS-1 rendered PC-12 cells resistant to H_2O_2 toxicity even in the absence of GDNF (Fig. 2), suggesting that NCS-1 itself is enough to promote cell survival. This is consistent with our view that NCS-1 is the downstream target for GDNF. Because growing evidence indicates that nerve injury leads to the up-regulation of multiple antiapoptotic molecules, including GDNF (Liberatore et al., 1997; Yamamoto et al., 1998; Wang et al., 2002), it is possible that neuronal damages induced by in vivo axotomy enhance the synthesis and/or secretion of GDNF, which, in turn, up-regulates NCS-1 expression and promotes neuronal survival in injured neurons. Although an underlying mechanism would be different, the up-regulation of NCS-1 has also been reported in the cortex of schizophrenic and bipolar patients, demonstrating the involvement of NCS-1 in neurological disease (Koh et al., 2003).

In conclusion, we characterized a novel function of NCS-1 mediating a GDNF-induced neuroprotective effect via activations of Akt kinase. Furthermore, we found that NCS-1 is up-regulated in response to nerve injury and plays an important role in the antiapoptotic mechanism in adult motor neurons. Our present findings would provide new and basic insights into the mechanism of neuronal regeneration.

Materials and methods

Plasmids and viral vectors

E120Q NCS-1 point mutant was generated with a conventional PCR protocol using the wild-type rat NCS-1 (GenBank/EMBL/DDBJ accession no. L27421 as a template and was sequenced to confirm the mutation.

Akt/PKBα cDNA was cloned from the human kidney cDNA library (CLONTECH Laboratories, Inc.), and NH_2-terminally tagged fluorescent protein EGFP-Akt/PKB-PH was constructed incorporating a fragment of 750 bp, encoding the first 250 amino acids of PKBα (containing the PH domain) into EGFP-vector as described previously (Currie et al., 1999).

Adenovirus containing wild-type NCS-1 and the E120Q mutant inserts were generated by cotransfecting either of these plasmids and pBHG11 (Microbix Biosystems, Inc.) into HEK 293 cells. Viral DNA was isolated from the supernatant in the wells displaying the cytopathic effect. Replication-incompetent virus containing DNA inserts were plaque-purified twice and grown on HEK 293 cells to produce large amounts of adenovirus. Tissue culture supernatant containing adenovirus was concentrated by centrifugation over cesium chloride. The titers of viral stocks were 2.2×10^{10} pfu/ml for EGFP–NCS-1, 1.1×10^{10} pfu/ml for EGFP-E120Q, and 2.2×10^{10} pfu/ml for EGFP-vector.

Cell cultures

PC-12 cells stably transfected with vector alone or vector containing cDNA coding for the wild-type NCS-1 (several clones) were grown onto collagen-coated (500 μg/ml of type I; Sigma-Aldrich) culture dishes in growth medium (DME containing 10% horse serum, 5% FBS, and 400 μg/ml geneticin and gentamicin) as described previously (Koizumi et al., 2002). When cells became 80% confluent, they were switched to the differentiation medium (growth medium with half serum) supplemented with 100 ng/ml NGF-7S (Invitrogen).

Primary culture of cortical neurons was performed using the cortex from Sprague-Dawley rats at embryonic day 18. In brief, cortical tissues were isolated from whole brain, minced into small pieces, and digested for 10 min at 37°C in a 20-U/ml papain solution containing 0.002% DNase I (Worthington Biochemical Corp.). After titration of the enzymatic activity, cells were mechanically dissociated by several passages through pipette tips. After centrifugation, cells were resuspended in neurobasal medium supplemented with B27 trophic factors (both from Invitrogen), whose compositions were reported previously (Brewer et al., 1993). They were then plated onto culture dishes coated with 0.1% polyethylenimine at a density of $2.5–5 \times 10^4$ cells/cm^2 for cell survival assay and 10^5 cells/cm^2 for immunoblot analysis.

Fluorescent microscopy

CCL39 cells and primary cultured rat cortical neurons were plated onto collagen-coated glass coverslips and cultivated for 1 d. They were then transiently transfected with the EGFP-Akt/PKB-PH construct together with either NCS-1, E120Q, or pCDNA3 (1:3 ratio) using LipofectAMINE 2000 (Invitrogen) and were subjected to immunocytochemistry. In brief, cells were fixed with 4% PFA, permeabilized with 0.2% Triton X-100, and blocked with 5% BSA. They were then incubated for 1 h with anti–NCS-1 antibody (1:200) followed by incubation with secondary antibodies (FITC- or rhodamine-conjugated goat anti–rabbit IgG; 1:200; Jackson ImmunoResearch Laboratories). After extensive wash with PBS, cell images were scanned on a laser confocal microscope (MRC-1024K; Bio-Rad Laboratories) or obtained with conventional epifluorescence illumination (BX50WI; Olympus) with a cooled CCD camera (CoolSNAP; Photometrics) using a 0.9-W 60× water immersion objective lens. Immunocytochemistry for PC-12 cells were also performed in the same way.

Evaluation of neuronal survival

The primary cultured neurons were infected with viruses at a multiplicity of infection of 100 pfu/cell at 5 d after plating. Under this condition, we found that nearly 70% of the neurons were infected by monitoring EGFP fluorescence (Fig. 3 A). The number of living neurons was counted within the fixed area of images taken by a digital camera (Coolpix 4500; Nikon). To count the number of cells always within the same area, a grid seal with numbering (Asahi Techno glass) was stuck on the bottom of each culture dish. The number of living neurons remaining at each day was expressed as a percentage of the initial number. Neurons showing the degenerating stage characterized by nuclear condensation, membrane blebbing, or extensive neurite fragmentation were excluded. Four different regions were selected from one dish, and six separate experiments were performed for each condition.

To identify and quantify apoptotic neurons, cells were fixed with 4% PFA and were stained with Hoechst 33258. Coverslips were mounted onto glass slides, and cells were observed under epifluorescence illumination on an inverted microscope (1X71; Olympus) using a 40× NA 1.35 oil immersion objective lens (Olympus). Cells were considered apoptotic if their nuclear chromatin was condensed or fragmented, whereas cells were considered viable if their chromatin was diffusely and evenly distributed throughout the nucleus (Fig. 3 F).

Immunoblot analysis

DMV tissue samples were obtained by scratching the DMV neurons from several frozen sections of brainstem (described in the next section) using pulled glass capillary under the light microscope. These tissue samples or cultured cells (PC-12 cells and cortical neurons) were then solubilized in SDS-PAGE sample buffer containing protease and phosphatase inhibitors and subjected to immunoblot analysis using image density software (Scion Image; Scion Corp.) as previously described (Nakamura et al., 2001). Primary antibodies used were anti–NCS-1 antibody (1:1,000), which was previously described (Jeromin et al., 1999), and publicly available antibodies: monoclonal anti-GAPDH antibody (1:1,000) obtained from Chemicon as well as antiphospho-Akt antibodies (detectable for the phosphorylation of Thr308 and Ser473; 1:1,000) and anti-Akt antibody (1:1,000; both from Cell Signaling Technology). Secondary antibodies used were HRP-conjugated anti–rabbit and anti–mouse antibodies or a combination of biotinylated anti–rabbit (or mouse) antibodies (Zymed Laboratories) and HRP-conjugated streptavidin (Zymed Laboratories).

In vivo axotomy and colchicine treatment

The method of vagus axotomy was described previously (Nabekura et al., 2002a). In brief, 4–6-wk-old Sprague-Dawley rats were deeply anesthetized with 50 mg/kg pentobarbital, and axotomy of the vagus motor neurons was performed with fine scissors at the unilateral vagus nerve at the neck. Injured neurons were confirmed by detecting the fluorescence of DiI in the DMV, which had been placed at the proximal cut site of the nerve bundle (Nabekura et al., 2002a).

To test the effects of colchicine, an implantable polymer containing 10% (wt/vol) colchicine was made by mixing colchicine with ethylene-vinyl acetate copolymer (Elvax) followed by drying as described previously (Kakizawa et al., 2000). Solid slices (~1 mm^2) were placed around the unilateral vagal nerve to allow the continuous release of colchicine from slices. The skin incision was closed, and rats were returned to the cage after awaking from the anesthetic.

Histology

1 d to 2 mo (usually 1 wk) after receiving ipsilateral vagal axotomy, brainstems were quickly removed, and 8–10-μm-thick frozen sections were cut. Immunohistochemistry was performed using the labeled biotin–streptavidin method. In brief, after fixation and blocking, the sections were incubated at 4°C overnight with a rabbit polyclonal antibody against NCS-1 at a dilution of 1:15,000 and were sequentially incubated with a biotinylated anti–rabbit secondary antibody and a HRP-conjugated streptavidin–biotin complex (GE Healthcare). The colored reaction product was developed with DAB solution. The sections were lightly counterstained with hematoxylin to visualize nuclei. Images were acquired using a digital camera (FX380; Olympus) equipped with an image filing software (FLVFS-LS; Flovel).

Comparison of the expression level of NCS-1 between injured and control sides were performed using computerized image analysis (Win Roof; Mitani Corp.). In brief, the DMV region from the injured side was at first selected, and the image was converted to binary images by thresholding so that only the area highly stained with anti–NCS-1 antibody could be detected. The same threshold level was used for both the control and injured DMV in each tissue section. The highly stained area was summated and represented as normalized values.

Neuronal degeneration was evaluated by counting surviving neurons as described previously (Rothstein et al., 2005) as well as by TUNEL staining using the apoptag peroxidase in situ Apoptosis Detection Kit (Chemicon). In brief, in vivo axotomy was performed as described above, and, at the same time, adenoviral vectors carrying EGFP only, EGFP plus NCS-1, or E120Q (10^9 pfu each) was injected into the stump of the nerve using a 34-gauge needle. 1 wk after axotomy, paraffin-embedded serial sections (3–4 μm) were made from the brainstem. After they were deparaffinized, sections were directly stained with hematoxylin/eosin to visualize the structure of the DMV region. TUNEL staining was performed in accordance with the manufacturer's method. The sections were lightly counterstained with methyl green. Control sections were treated similarly but incubated in the absence of TdT enzyme. To confirm whether the adenoviral vectors were transferred to the DMV neurons, another set of animals were treated in the same way. 8-μm frozen sections were cut 1 wk after operation, and EGFP signals were viewed under a fluorescence microscope (1X71; Olympus). All image acquisitions were performed at room temperature, and images were subsequently processed using Adobe Photoshop (version 7) and Adobe Illustrator (version 10) software. All experiments conformed to the Guiding Principles for the Care and Use of Animals approved by the Council of the Physiological Society of Japan. All efforts were made to minimize the number of animals used and their suffering.

Statistics

Comparisons between two groups were performed using the paired or unpaired *t* test. Values of $P < 0.05$ were considered statistically significant. All summarized data are expressed as means ± SEM.

We thank Dr. Andrew Moorhouse (The University of New South Wales, Sydney, Australia) for critical reading of this manuscript. We also thank Dr. Takeharu Nishimoto and Dr. Hideo Nishitani (Kyushu University, Fukuoka, Japan) for useful discussions of this study.

This work was supported, in part, by a Grant-in-Aid for Scientific Research (17590196) and Priority Areas (13142210) from the Ministry of Education, Culture, Sports, Science and Technology of Japan and the Japan Heart Foundation and by a grant from the National Institutes of Health/National Institute of Neurological Disorder and Stroke (NS38126).

Submitted: 24 August 2005
Accepted: 17 February 2006

References

Alessi, D.R., M. Andjelkovic, B. Caudwell, P. Cron, N. Morrice, P. Cohen, and B.A. Hemmings. 1996. Mechanism of activation of protein kinase B by insulin and IGF-1. *EMBO J.* 15:6541–6551.

Benn, S.C., and C.J. Woolf. 2004. Adult neuron survival strategies–slamming on the brakes. *Nat. Rev. Neurosci.* 5:686–700.

Boyd, J.G., and T. Gordon. 2003. Neurotrophic factors and their receptors in axonal regeneration and functional recovery after peripheral nerve injury. *Mol. Neurobiol.* 27:277–324.

Brewer, G.J. 1995. Serum-free B27/neurobasal medium supports differentiated growth of neurons from the striatum, substantia nigra, septum, cerebral cortex, cerebellum, and dentate gyrus. *J. Neurosci. Res.* 42:674–683.

Brewer, G.J., J.R. Torricelli, E.K. Evege, and P.J. Price. 1993. Optimized survival of hippocampal neurons in B27-supplemented Neurobasal, a new serum-free medium combination. *J. Neurosci. Res.* 35:567–576.

Cantley, L.C. 2002. The phosphoinositide 3-kinase pathway. *Science.* 296:1655–1657.

Chen, X.L., Z.G. Zhong, S. Yokoyama, C. Bark, B. Meister, P.O. Berggren, J. Roder, H. Higashida, and A. Jeromin. 2001. Overexpression of rat neuronal calcium sensor-1 in rodent NG108-15 cells enhances synapse formation and transmission. *J. Physiol.* 532:649–659.

Cheng, A., S. Wang, D. Yang, R. Xiao, and M.P. Mattson. 2003. Calmodulin mediates brain-derived neurotrophic factor cell survival signaling upstream of Akt kinase in embryonic neocortical neurons. *J. Biol. Chem.* 278:7591–7599.

Currie, R.A., K.S. Walker, A. Gray, M. Deak, A. Casamayor, C.P. Downes, P. Cohen, D.R. Alessi, and J. Lucocq. 1999. Role of phosphatidylinositol 3,4,5-trisphosphate in regulating the activity and localization of 3-phosphoinositide-dependent protein kinase-1. *Biochem. J.* 337:575–583.

Gomez, M., E. De Castro, E. Guarin, H. Sasakura, A. Kuhara, I. Mori, T. Bartfai, C.I. Bargmann, and P. Nef. 2001. Ca^{2+} signaling via the neuronal calcium sensor-1 regulates associative learning and memory in *C. elegans*. *Neuron.* 30:241–248.

Henderson, C.E., H.S. Phillips, R.A. Pollock, A.M. Davies, C. Lemeulle, M. Armanini, L. Simmons, B. Moffet, R.A. Vandlen, L.C. Simpson, et al. 1994. GDNF: a potent survival factor for motoneurons present in peripheral nerve and muscle. *Science.* 266:1062–1064.

Hendricks, K.B., B.Q. Wang, E.A. Schnieders, and J. Thorner. 1999. Yeast homologue of neuronal frequenin is a regulator of phosphatidylinositol-4-OH kinase. *Nat. Cell Biol.* 1:234–241.

Jeromin, A., A.J. Shayan, M. Msghina, J. Roder, and H.L. Atwood. 1999. Crustacean frequenins: molecular cloning and differential localization at neuromuscular junctions. *J. Neurobiol.* 41:165–175.

Jeromin, A., D. Muralidhar, M.N. Parameswaran, J. Roder, T. Fairwell, S. Scarlata, L. Dowal, S.M. Mustafi, K.V. Chary, and Y. Sharma. 2004. N-terminal myristoylation regulates calcium-induced conformational changes in neuronal calcium sensor-1. *J. Biol. Chem.* 279:27158–27167.

Kakizawa, S., M. Yamasaki, M. Watanabe, and M. Kano. 2000. Critical period for activity-dependent synapse elimination in developing cerebellum. *J. Neurosci.* 20:4954–4961.

Kirik, D., B. Georgievska, and A. Bjorklund. 2004. Localized striatal delivery of GDNF as a treatment for Parkinson disease. *Nat. Neurosci.* 7:105–110.

Kiryu-Seo, S., M. Sasaki, H. Yokohama, S. Nakagomi, T. Hirayama, S. Aoki, K. Wada, and H. Kiyama. 2000. Damage-induced neuronal endopeptidase (DINE) is a unique metallopeptidase expressed in response to neuronal damage and activates superoxide scavengers. *Proc. Natl. Acad. Sci. USA.* 97:4345–4350.

Koh, P.O., A.S. Undie, N. Kabbani, R. Levenson, P.S. Goldman-Rakic, and M.S. Lidow. 2003. Up-regulation of neuronal calcium sensor-1 (NCS-1) in the prefrontal cortex of schizophrenic and bipolar patients. *Proc. Natl. Acad. Sci. USA.* 100:313–317.

Koizumi, S., P. Rosa, G.B. Willars, R.A. Challiss, E. Taverna, M. Francolini, M.D. Bootman, P. Lipp, K. Inoue, J. Roder, and A. Jeromin. 2002. Mechanisms underlying the neuronal calcium sensor-1-evoked enhancement of exocytosis in PC12 cells. *J. Biol. Chem.* 277:30315–30324.

Korhonen, L., I. Hansson, J.P. Kukkonen, K. Brannvall, M. Kobayashi, K. Takamatsu, and D. Lindholm. 2005. Hippocalcin protects against caspase-12-induced and age-dependent neuronal degeneration. *Mol. Cell. Neurosci.* 28:85–95.

Liberatore, G.T., J.Y. Wong, M.J. Porritt, G.A. Donnan, and D.W. Howells. 1997. Expression of glial cell line-derived neurotrophic factor (GDNF) mRNA following mechanical injury to mouse striatum. *Neuroreport.* 8:3097–3101.

Liston, P., W.G. Fong, and R.G. Korneluk. 2003. The inhibitors of apoptosis: there is more to life than Bcl2. *Oncogene.* 22:8568–8580.

Mallart, A., D. Angaut-Petit, C. Bourret-Poulain, and A. Ferrus. 1991. Nerve terminal excitability and neuromuscular transmission in T(X;Y)V7 and Shaker mutants of *Drosophila melanogaster*. *J. Neurogenet.* 7:75–84.

Mercer, E.A., L. Korhonen, Y. Skoglosa, P.A. Olsson, J.P. Kukkonen, and D. Lindholm. 2000. NAIP interacts with hippocalcin and protects neurons against calcium-induced cell death through caspase-3-dependent and -independent pathways. *EMBO J.* 19:3597–3607.

Nabekura, J., T. Ueno, S. Katsurabayashi, A. Furuta, N. Akaike, and M. Okada. 2002a. Reduced NR2A expression and prolonged decay of NMDA receptor-mediated synaptic current in rat vagal motoneurons following axotomy. *J. Physiol.* 539:735–741.

Nabekura, J., T. Ueno, A. Okabe, A. Furuta, T. Iwaki, C. Shimizu-Okabe, A. Fukuda, and N. Akaike. 2002b. Reduction of KCC2 expression and GABAA receptor-mediated excitation after in vivo axonal injury. *J. Neurosci.* 22:4412–4417.

Nakamura, T.Y., D.J. Pountney, A. Ozaita, S. Nandi, S. Ueda, B. Rudy, and W.A. Coetzee. 2001. A role for frequenin, a Ca^{2+}-binding protein, as a regulator of Kv4 K^+-currents. *Proc. Natl. Acad. Sci. USA.* 98:12808–12813.

Nakamura, T.Y., E. Sturm, D.J. Pountney, B. Orenzoff, M. Artman, and W.A. Coetzee. 2003. Developmental expression of NCS-1 (frequenin), a regulator of Kv4 K^+ channels, in mouse heart. *Pediatr. Res.* 53:554–557.

Nicole, O., C. Ali, F. Docagne, L. Plawinski, E.T. MacKenzie, D. Vivien, and A. Buisson. 2001. Neuroprotection mediated by glial cell line-derived neurotrophic factor: involvement of a reduction of NMDA-induced calcium influx by the mitogen-activated protein kinase pathway. *J. Neurosci.* 21:3024–3033.

Olafsson, P., T. Wang, and B. Lu. 1995. Molecular cloning and functional characterization of the *Xenopus* Ca^{2+}-binding protein frequenin. *Proc. Natl. Acad. Sci. USA.* 92:8001–8005.

Oppenheim, R.W., L.J. Houenou, J.E. Johnson, L.F. Lin, L. Li, A.C. Lo, A.L. Newsome, D.M. Prevette, and S. Wang. 1995. Developing motor neurons rescued from programmed and axotomy-induced cell death by GDNF. *Nature.* 373:344–346.

Perez-Garcia, M.J., V. Cena, Y. de Pablo, M. Llovera, J.X. Comella, and R.M. Soler. 2004. Glial cell line-derived neurotrophic factor increases intracellular calcium concentration. Role of calcium/calmodulin in the activation of the phosphatidylinositol 3-kinase pathway. *J. Biol. Chem.* 279:6132–6142.

Perrelet, D., A. Ferri, P. Liston, P. Muzzin, R.G. Korneluk, and A.C. Kato. 2002. IAPs are essential for GDNF-mediated neuroprotective effects in injured motor neurons in vivo. *Nat. Cell Biol.* 4:175–179.

Pongs, O., J. Lindemeier, X.R. Zhu, T. Theil, D. Engelkamp, I. Krah-Jentgens, H.G. Lambrecht, K.W. Koch, J. Schwemer, R. Rivosecchi, et al. 1993. Frequenin–a novel calcium-binding protein that modulates synaptic efficacy in the *Drosophila* nervous system. *Neuron.* 11:15–28.

Rothstein, J.D., S. Patel, M.R. Regan, C. Haenggeli, Y.H. Huang, D.E. Bergles, L. Jin, M. Dykes Hoberg, S. Vidensky, D.S. Chung, et al. 2005. Beta-lactam antibiotics offer neuroprotection by increasing glutamate transporter expression. *Nature.* 433:73–77.

Sippy, T., A. Cruz-Martin, A. Jeromin, and F.E. Schweizer. 2003. Acute changes in short-term plasticity at synapses with elevated levels of neuronal calcium sensor-1. *Nat. Neurosci.* 6:1031–1038.

Soler, R.M., X. Dolcet, M. Encinas, J. Egea, J.R. Bayascas, and J.X. Comella. 1999. Receptors of the glial cell line-derived neurotrophic factor family of neurotrophic factors signal cell survival through the phosphatidylinositol 3-kinase pathway in spinal cord motoneurons. *J. Neurosci.* 19:9160–9169.

Takahashi, M. 2001. The GDNF/RET signaling pathway and human diseases. *Cytokine Growth Factor Rev.* 12:361–373.

Tsujimoto, T., A. Jeromin, N. Saitoh, J.C. Roder, and T. Takahashi. 2002. Neuronal calcium sensor 1 and activity-dependent facilitation of P/Q-type calcium currents at presynaptic nerve terminals. *Science.* 295:2276–2279.

Wang, C.Y., F. Yang, X. He, A. Chow, J. Du, J.T. Russell, and B. Lu. 2001. Ca^{2+} binding protein frequenin mediates GDNF-induced potentiation of Ca^{2+} channels and transmitter release. *Neuron.* 32:99–112.

Wang, Y., C.F. Chang, M. Morales, Y.H. Chiang, and J. Hoffer. 2002. Protective effects of glial cell line-derived neurotrophic factor in ischemic brain injury. *Ann. NY Acad. Sci.* 962:423–437.

Weiss, J.L., D.A. Archer, and R.D. Burgoyne. 2000. Neuronal Ca^{2+} sensor-1/frequenin functions in an autocrine pathway regulating Ca^{2+} channels in bovine adrenal chromaffin cells. *J. Biol. Chem.* 275:40082–40087.

Weisz, O.A., G.A. Gibson, S.M. Leung, J. Roder, and A. Jeromin. 2000. Overexpression of frequenin, a modulator of phosphatidylinositol 4-kinase, inhibits biosynthetic delivery of an apical protein in polarized madin-darby canine kidney cells. *J. Biol. Chem.* 275:24341–24347.

Yamamoto, M., N. Mitsuma, Y. Ito, N. Hattori, M. Nagamatsu, M. Li, T. Mitsuma, and G. Sobue. 1998. Expression of glial cell line-derived neurotrophic factor and GDNFR-alpha mRNAs in human peripheral neuropathies. *Brain Res.* 809:175–181.

Yan, Q., C. Matheson, and O.T. Lopez. 1995. In vivo neurotrophic effects of GDNF on neonatal and adult facial motor neurons. *Nature.* 373:341–344.

European Journal of Neuroscience, Vol. 24, pp. 2135–2144, 2006 doi:10.1111/j.1460-9568.2006.05092.x

BDNF occludes $GABA_B$ receptor-mediated inhibition of GABA release in rat hippocampal CA1 pyramidal neurons

Yoshito Mizoguchi,[1,*] Akihiko Kitamura,[1,2,*] Hiroaki Wake,[1] Hitoshi Ishibashi,[3] Miho Watanabe,[1] Takuya Nishimaki[1,4] and Junichi Nabekura[1,2,4]

[1]Division of Homeostatic Development, Department of Developmental Physiology, National Institute of Physiological Sciences, 38 Myodaiji, Okazaki 444-8585 Japan

[2]CREST, the Japan Science and Technology Corporation, 4-1-8 Honcho, Kawaguchi, Saitama 332-0012, Japan

[3]Department of Cellular Physiology, Faculty of Medicine Kyushu University, 3-1-1 Maidashi, Higashiku, Fukuoka, 812-8582, Japan

[4]Department of Biological Sciences, Sokendai, 38 Myodaiji, Okazaki 444-8585, Japan

Keywords: BDNF, $GABA_B$ receptor, hippocampus, protein kinase C, pyramidal neuron, TrkB receptor tyrosine kinase

Abstract

During the development of the rat hippocampus, both γ-aminobutyric acid $(GABA)_B$ autoreceptors and brain-derived neurotrophic factor (BDNF) play important roles in the formation of GABAergic synapses as well as in the $GABA_A$ receptor-mediated transmissions. While a number of studies have reported rapid effects of BDNF on $GABA_A$ receptor-mediated responses, the interactions between $GABA_B$ autoreceptors and BDNF are less clear. Using conventional whole-cell patch-clamp recordings, we demonstrated here that BDNF significantly occludes baclofen-induced suppression of $GABA_A$ receptor-mediated transmissions in each of the preparations including hippocampal slices prepared from P14 rats, hippocampal CA1 pyramidal neurons isolated from P14 and P21 rats, and cultured hippocampal pyramidal neurons. This effect of BDNF was rapid and reversible, and was mediated via the activation of presynaptic TrkB receptor tyrosine kinases, and subsequent activation of phospholipase C and protein kinase C. On the contrary, in hippocampal CA1 pyramidal neurons isolated from P7 rats, BDNF failed to occlude the $GABA_B$ receptor-mediated inhibition of GABA release. Thus, the ability of BDNF to occlude the $GABA_B$ receptor-mediated inhibition of GABA release develops between P7 and P14. This demonstrates a novel aspect of the effects of BDNF on inhibitory transmissions in rat hippocampus, which may have some functional roles in the induction of developmental plasticity and/or pathophysiology of epilepsy.

Introduction

Brain-derived neurotrophic factor (BDNF) is a neurotrophin best known for its role in inducing long-term functional and structural alterations in neurons, synapses and neuronal circuits during development of the CNS (Katz & Shatz, 1996; Poo, 2001; Lu, 2003). In hippocampal cultures, long-term exposure to BDNF or overexpression of BDNF results in an earlier maturation of inhibitory synapses by inducing both presynaptic and postsynaptic structural and functional modifications to enhance γ-aminobutyric acid (GABA)ergic transmission (Vicario-Abejón *et al.*, 1998; Marty *et al.*, 2000; Yamada *et al.*, 2002).

These trophic effects of BDNF on GABAergic transmission generally occur over a time-course of hours to days. However, acute application of BDNF can result in sustained modulation of GABAergic transmission, although the reported effects vary due to the type of neuron recorded from (Wardle & Poo, 2003) and the developmental stage of the animal (Mizoguchi *et al.*, 2003a). In hippocampal pyramidal neurons from 1-week-old rats, BDNF potentiates inhibitory responses, with both presynaptic enhancement of GABA release (Gubellini *et al.*, 2005) and an enhanced postsynaptic $GABA_A$ receptor-mediated response (Mizoguchi *et al.*, 2003a). In hippocampal neurons in older rats, BDNF has generally been reported to inhibit $GABA_A$ receptor responses, although the underlying mechanisms are not totally clear with both postsynaptic (Tanaka *et al.*, 1997; Brünig *et al.*, 2001; Mizoguchi *et al.*, 2003a; Jovanovic *et al.*, 2004) and presynaptic (Frerking *et al.*, 1998; Poo, 2001) mechanisms implicated in different studies.

Presynaptic $GABA_B$ receptors are distributed widely throughout the brain where their activation results in inhibition of transmitter release, primarily through inhibition of presynaptic Ca^{2+} channels (Misgeld *et al.*, 1995). At GABAergic transmissions, they can act as autoreceptors to reduce GABA release (Misgeld *et al.*, 1995; Nicoll, 2004). In the hippocampal slice from $GABA_BR1$ knockout mice, for example, the presynaptic inhibition of evoked $GABA_A$ receptor-mediated currents is absent (Prosser *et al.*, 2001). The knockout mice also demonstrate the importance of $GABA_B$ receptors during development; mice develop normally until P9 after which they develop severe seizures and die at about P27 (Prosser *et al.*, 2001).

Despite intensive investigation of the effects of BDNF on $GABA_A$ receptor-mediated transmission, there have been no prior reports on how BDNF affects signaling via $GABA_B$ receptors, which is somewhat surprising considering their important roles in neuronal function (Davies *et al.*, 1991; Bettler *et al.*, 2004). In the present study,

Correspondence: Dr J. Nabekura, [1]Division of Homeostatic Development, as above.
E-mail: nabekura@nips.ac.jp

*Y.M. and A.K. contributed equally to this work.

Received 15 January 2006, revised 31 July 2006, accepted 2 August 2006

we examined the acute effects of BDNF on $GABA_B$ autoreceptors function in rat hippocampal CA1 pyramidal neurons during development.

Materials and methods

All experiments conformed to the Guiding Principles for the Care and Use of Animals approved by the Council of the Physiological Society of Japan and the United States National Institutes of Health Guide for the Care and Use of Laboratory Animals. All efforts were made to minimize the number of animals used.

Whole-cell recording from hippocampal slices

Wistar rats, at postnatal day (P)13–16 were used for slice experiments. Rats were deeply anesthetized with isoflurane (Abbott, Abbott Park, IL, USA) and then decapitated. Coronal slices containing the CA1 regions of hippocampus were made as previously described (Mizoguchi *et al.*, 2003a). Briefly, coronal slices of the hippocampus (300 μm thickness) were obtained using a vibrating blade microtome (VT-1000; Leica; Nussloch; Germany). For the recording of evoked inhibitory postsynaptic currents (eIPSCs), a single slice was transferred to a submerged chamber and was perfused continuously with an external artificial cerebrospinal fluid (ACSF) at 28 ± 1 °C that was composed of the following (in mM): NaCl, 120; KCl, 2; KH_2PO_4, 1; $CaCl_2$, 2; $MgCl_2$, 1; $NaHCO_3$, 26; glucose, 10; bubbled with a mixture of 95% O_2/5% CO_2 (pH 7.4). The flow rate of the ACSF was 2 mL/min.

The conventional whole-cell recordings were performed with a blind approach. Patch pipettes (4–6 MΩ) were filled with a solution containing (in mM): Cs methane sulfonate, 130; CsCl, 5; EGTA, 0.6; tetraethylammonium (TEA)-Cl, 5; ATP-Mg, 4; GDP-beta-S, 0.3; HEPES, 10; and adjusted to pH 7.2 by Tris-OH. Current and voltage were recorded with a patch-clamp amplifier (MultiClamp 700B; Axon Instruments, Foster City, USA), filtered at 1 kHz, digitized at a rate of 4 kHz and fed into a computer for analysis. Voltage-clamp recordings were performed at a pipette potential of 0 mV. The series resistance (usually 10–25 MΩ) was periodically monitored by delivering −10 mV hyperpolarizing step pulses. Data were only obtained during continuous recordings in which the series resistance did not change by > 15%. eIPSCs were obtained by stratum radiatum stimulation at every 15 s with a glass pipette electrode. 6 cyano-nitroquinoxaline-2,3-dione (CNQX, 10 μM) and 2-amino-5-phosphonopentanoic acid (APV, 40 μM) were included in ACSF for all recordings from slices. Human recombinant BDNF (Sigma, St Louis, MO, USA) was dissolved (10 μg/mL) in phosphate buffer solution containing 0.1% bovine serum albumin and stored below −20 °C. Just prior to an experiment, this stock solution was diluted with ACSF to obtain the final concentration (50 ng/mL).

Recording from dissociated hippocampal neurons

Wistar rats, at P 6–7, P13–16 and P21–22 were used for the recording from dissociated neurons (henceforth referred to as P7, P14 and P21 rats, respectively). Single hippocampal pyramidal neurons were acutely dissociated from brain slices, so as to preserve functional presynaptic nerve terminals adherent to the isolated neurons (Nabekura *et al.*, 2004). Rats were decapitated under pentobarbital anesthesia (50 mg/kg, i.p.). Coronal slices containing the CA1 regions of hippocampus were made as previously described (Mizoguchi *et al.*, 2003a). Briefly, brains were quickly removed and transversely sliced at a thickness of 370 μm (VT-1000; Leica) in an ice-cold oxygenated cutting solution containing (in mM): sucrose, 248; KCl, 2; $MgSO_4$, 2; KH_2PO_4, 1.25; $CaCl_2$, 1; $MgCl_2$, 1; $NaHCO_3$, 26; glucose, 10; pH 7.4, equilibrated with 95% O_2 and 5% CO_2, and with an osmolality of 340 mOsm/L. Slices were then transferred to an incubation medium (see below) saturated with 95% O_2 and 5% CO_2 at room temperature of 28 ± 1 °C for at least 1.5 h. Following this, a slice was transferred into a 35-mm culture dish (Primaria; Falcon, Lincoln Park, NJ, USA), containing standard external solution (see below), and the CA1 region of the hippocampus was identified under a binocular microscope (× 20, SMZ-1; Nikon, Tokyo, Japan). A fire-polished blunt glass pipette was touched lightly onto the surface of the stratum pyramidale of the CA1 region and vibrated horizontally at a frequency of 30–50 Hz and with an amplitude of 0.05 mm for 1 min, using a custom-built vibration apparatus. Slices were gently removed from the dish and dissociated neurons adhered to the bottom of the dish within 15 min. Only neurons with a pyramidal-shaped soma, a prominent apical dendrite and additional dendrites were used for the recordings.

Cultured hippocampal neurons were prepared from embryonic day (E)18–E20 Wistar rat embryos. Hippocampi were incubated with trypsin for 20 min at 37 °C and then gently triturated. Dissociated neurons were plated at 50 000–80 000 cells/cm^2 on polyethyleneimine-coated glass coverslips and subsequently incubated in Dulbecco's modified essential medium supplemented with 10% fetal bovine serum and 50 U/mL penicillin-streptomycin (all from Sigma). Twenty-four hours after plating the medium was changed to Neurobasal-A/B (Invitron, Carlsbad, CA, USA), and the neurons were subsequently maintained in culture for 14–17 days [14–17 days *in vitro* (DIV)] before recordings.

Electrical measurements were performed using either the nystatin-perforated patch recording mode or the conventional whole-cell recording method. Patch pipettes were made from borosilicate capillary glass tubes (G-1.5; Narishige, Tokyo, Japan) in two stages on a vertical pipette puller (PB-7; Narishige). The tip resistance of the electrodes was 4–6 MΩ. Neurons were visualized with phase contrast equipment on an inverted microscope (Diaphoto; Nikon). Current and voltage were recorded with a patch-clamp amplifier (EPC-7; List Biologic, Campbell, CA, USA), continuously monitored on an oscilloscope (VC-6725; Hitachi, Tokyo, Japan) and a pen recorder (Recti-Horiz-8K; Sanei, Tokyo, Japan), and recorded on a digital-audio tape recorder (RD-120TE; TEAC). Voltage-clamp recordings were performed at a pipette potential of −50 mV for nystatin-perforated patch recordings and at −60 mV for the conventional whole-cell recordings. Membrane currents were filtered at 1 kHz (E-3201 A Decade Filter; NF Electronic Instruments, Tokyo, Japan) and data were digitized at 4 kHz and stored on a computer equipped with pCLAMP 8.0 (Axon Instruments, Union City, CA, USA). The access resistance was periodically monitored by delivering −10 mV hyperpolarizing step pulses. Data were only obtained during continuous recordings in which the series resistance did not change by > 15%.

Miniature (m)IPSCs were acquired using pClamp 8.0, and analysed using both pClamp 8.0 and MiniAnalysis (Synaptosoft, NJ, USA). Individual events were detected using an amplitude threshold fourfold greater than the mean root-square-noise level (which ranged from 0.8 to 4.3 pA in this study), and then detected events were rejected or accepted on the basis of their rise and decay times in each experiment. When two or more events overlapped, the baseline current of the latter event was calculated by extrapolating the decay phase of the preceding event to baseline. Only data from neurons in which a large number of mIPSCs (> 1000) were obtained were further analysed. All data are expressed as mean ± SEM, and statistical analysis was performed using Student's *t*-test, with $P < 0.05$ being considered significantly different. Cumulative distribution plots of the frequency of mIPSCs

were also generated and compared using the Kolmogorov–Smirnov test.

The electrode solution for nystatin-perforated patch recordings contained (in mM): methanesulfonic acid potassium salt, 40; KCl, 110; HEPES, 10. The pH of these internal solutions was adjusted to 7.2 with Tris-OH. Nystatin (Sigma) was dissolved in acidified methanol at 10 mg/mL. This stock solution was diluted with internal pipette solution just before use to a final concentration of 100–200 μg/mL. For conventional whole-cell recordings, electrodes were filled with the following solution (in mM): methanesulfonic acid cesium salt, 80; CsCl, 70; $CaCl_2$, 0.2; EGTA, 2; TEA-Cl, 5; ATP-Mg, 5; HEPES, 10. The pH of these internal solutions was adjusted to 7.2 with Tris-OH. The ionic composition of the incubation medium for the hippocampal slices was (in mM): NaCl, 124; KCl, 5; KH_2PO_4, 1.2; $NaHCO_3$, 24; $CaCl_2$, 2.4; $MgSO_4$, 1.3; glucose, 10. Following equilibration with 95% O_2–5% CO_2, the pH was 7.4. The ionic composition of the standard external solution was (in mM): NaCl, 150; KCl, 5; $CaCl_2$, 2; $MgCl_2$, 1; glucose, 10; HEPES, 10. The pH of the standard external solution was also adjusted to 7.4 with Tris-OH. Drug solutions were applied using a Y-tube perfusion system, allowing rapid exchange of the solution surrounding a cell (e.g. Nabekura *et al.*, 2002).

The drugs used in the present study included baclofen, APV, CNQX, bicuculline, U73122, calphostin C, GDP-beta-S and phorbol-12,13-dibutyrate (PDBu, all from Sigma), tetrodotoxin (TTX; Wako, Tokyo, Japan), K252a, anti-tyrosine receptor kinase (Trk) B (Ab-1) polyclonal antibody (Calbiochem, La Jolla, CA, USA) and CGP55845A (Novartis Pharma, Basal, Switzerland). Drugs that were insoluble in water were first dissolved in dimethylsulfoxide (DMSO) and then diluted in the standard external solution. The final concentration of DMSO was always less than 0.1%. TTX (300 nM), CNQX (10 μM) and APV (20 μM) were included in the standard external solution for all recordings from dissociated neurons. Human recombinant BDNF (Sigma) was diluted with the standard external solution to obtain the final concentration (20 ng/mL). This BDNF concentration is sufficient to promote neurite outgrowth and the establishment of functional inhibitory synaptic connections in cultured hippocampal neurons (Vicario-Abejón *et al.*, 1998), and acutely modulates postsynaptic $GABA_A$ receptor-mediated currents in rat hippocampal CA1 pyramidal neurons (Tanaka *et al.*, 1997; Mizoguchi *et al.*, 2003a) and in rat visual cortical pyramidal neurons (Mizoguchi *et al.*, 2003b).

Results

Lack of postsynaptic $GABA_B$ responses in CA1 neurons acutely isolated from P14 rats

Dissociated neurons are used to measure postsynaptic (Mizoguchi *et al.*, 2002, 2003a) or spontaneous synaptic (Kakazu *et al.*, 1999; Zhu & Lovinger, 2005) currents under good space-clamp conditions and without complications from surrounding neurons or glia.

Pyramidal neurons were acutely isolated from the stratum pyramidale of the hippocampal CA1 region in P14 rats. Voltage-clamp recordings were obtained at a holding potential of −50 mV, using nystatin-perforated patch-clamp recordings, which preserve divalent ions and other intracellular constituents intact (Horn & Marty, 1988).

In hippocampal pyramidal neurons from adult rats, the application of the selective $GABA_B$ receptor agonist, baclofen, induces a potassium current (Bowery *et al.*, 2002) with an EC_{50} of about 3 μM (Sodickson & Bean, 1996). However, in hippocampal CA1 pyramidal neurons isolated from P14 rats, the application of baclofen (10–100 μM; treatment for 3–5 min) never caused any change in the holding current ($n = 6$ from four rats; Fig. 1A), consistent with the report that significant postsynaptic $GABA_B$ receptor-mediated currents are observed only at later developmental stage (> P23, Nurse & Lacaille, 1999), possibly due to a lack of coupling between $GABA_B$ receptors and their associated G-proteins and effector K^+ channels (Ben-Ari *et al.*, 1997). In the same six neuron recordings, the application of baclofen in the presence of BDNF (20 ng/mL) again had no effect on the holding current, indicating that BDNF dose not induce any precocious postsynaptic $GABA_B$ receptor-mediated responses in CA1 pyramidal neurons from P14 rats.

BDNF reversibly occludes presynaptic $GABA_B$ receptor-mediated inhibition of GABA release in both acutely isolated and cultured hippocampal CA1 neurons

Functional presynaptic $GABA_B$ receptors mature much earlier than postsynaptic $GABA_B$ receptors (Ben-Ari *et al.*, 1997) and act as GABA autoreceptors at presynaptic inhibitory GABAergic terminals to reduce GABA release (Nicoll, 2004). To clearly isolate actions of presynaptic $GABA_B$ receptor activation, we used conventional whole-cell patch-clamp recordings at a holding potential of −60 mV, using a pipette solution that contained GDP-beta-S (300 μM; a G-protein hydrolysis inhibitor that blocks postsynaptic G-protein activation) and with K^+ replaced by Cs^+ and TEA (to block postsynaptic K^+ channels). Firstly, using isolated CA1 pyramidal neurons from P14 rats, we recorded spontaneous mIPSCs in the presence of 10 μM CNQX, 20 μM APV and 300 nM TTX. Furthermore, we confirmed mIPSCs were $GABA_A$ receptor-mediated because they were completely and reversibly blocked by 10 μM bicuculline ($n = 5$, data not shown). The mean frequency and amplitude of spontaneous GABAergic mIPSCs recorded under these conditions were 1.72 ± 0.28 Hz and 39.0 ± 5.1 pA, respectively ($n = 56$ from 39 rats). These values are similar to those previously reported (e.g. Cohen *et al.*, 2000; De Simoni *et al.*, 2003).

In rat hippocampal CA1 pyramidal neurons, baclofen reduces the frequency of mIPSCs with an EC_{50} of 18 μM (Jarolimek & Misgeld, 1997). We used an almost saturating concentration of 10 μM in all experiments with acutely isolated and cultured neurons. This concentration of baclofen profoundly decreased the frequency of mIPSCs (to 52.4 ± 8.4% of the control; $n = 13$ from eight rats; e.g. Fig. 1A, mean data in Fig. 2), without causing any change in the current amplitude (which was 95.7 ± 6.4% of the pre-baclofen control, $P = 0.20$). The averaged mIPSC frequency recovered back to control values within 3 min of washing out baclofen (Fig. 2). The inhibitory effect of baclofen on mIPSCs frequency was completely abolished by 3 μM CGP55845A, a selective $GABA_B$ receptor antagonist (Misgeld *et al.*, 1995; $n = 5$; data not shown).

We next tested the effect of BDNF on this presynaptic $GABA_B$ receptor-mediated inhibition of GABA release. In the presence of BDNF (20 ng/mL), 10 μM baclofen failed to cause any reduction in the frequency of mIPSCs, which was, on average, 98.0 ± 7.7% of the mIPSC frequency in the presence of BDNF and before the addition of baclofen ($n = 11$ from eight rats; e.g. Fig. 1B, mean data in Fig. 2). These results indicate that BDNF occludes the presynaptic $GABA_B$ receptor-mediated inhibition of GABA release from terminals synapsing on to hippocampal CA1 pyramidal neurons isolated from P14 rats.

We and others have previously reported that a brief application of BDNF induces a sustained inhibition of postsynaptic $GABA_A$ receptor-mediated currents in hippocampal CA1 pyramidal neurons from P14 rats, which persists following the washout of BDNF (Tanaka

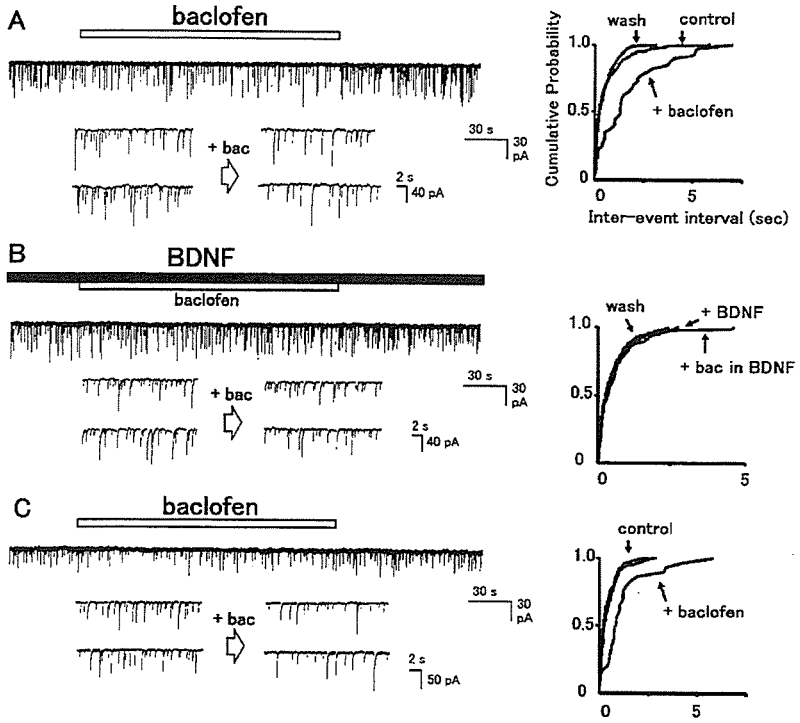

FIG. 1. Effects of baclofen and brain-derived neurotrophic factor (BDNF) on mIPSCs in a hippocampal CA1 pyramidal neuron isolated from P14 rats. (A–C) Representative current traces (left, upper), and current traces with an expanded time scale (left, lower), demonstrating that 10 μM baclofen application inhibits mIPSC frequency in control conditions (A) and following BDNF washout (C), but fails to effect mIPSC frequency in the continued presence of 20 ng/mL BDNF (B). Downward deflections represent $GABA_A$ receptor-mediated mIPSCs. Note the lack of effect of 10 μM baclofen application on the holding current in (A–C). Corresponding cumulative mIPSC frequency distributions recorded in each condition are also shown (right; A, control vs. + baclofen, $P < 0.01$, K–S-test; B, + BDNF vs. + baclofen in BDNF, $P = 0.52$, K–S-test; C, control vs. + baclofen, $P < 0.01$, K–S-test).

et al., 1997; Mizoguchi *et al.*, 2003a). In the present study, we also confirmed that BDNF by itself inhibited the amplitude of mIPSCs, to 71.3 ± 9.2% of the pre-BDNF control ($P = 0.03$), without affecting mean mIPSC frequency (which was 93.5 ± 7.1% of the pre-BDNF control, $P = 0.21$; Fig. 2). The co-application of baclofen did not change mIPSC amplitude (70.4 ± 4.0% of the pre-BDNF control). The inhibition of mIPSC amplitude persisted following BDNF washout, being 62.9 ± 10.1% of the pre-BDNF control after 10 min of BDNF washout (not shown).

In contrast to the sustained decrease in mIPSC amplitude, BDNF occlusion of the baclofen response was readily reversible. After washout of BDNF, baclofen (10 μM) again significantly decreased mIPSCs frequency, to 50.4 ± 9.8% of the control ($n = 6$; Fig. 1C, see also Fig. 2), which was almost identical to the mean inhibition prior to BDNF application.

One possible reason underlying the diversity of acute BDNF actions on $GABA_A$ receptor-mediated transmission in the CNS (see Introduction) could be differences in neuronal preparations. We therefore also tested the effects of BDNF on $GABA_B$ receptor-mediated inhibition of GABA release using cultured hippocampal pyramidal neurons (14–17 DIV), a preparation commonly used for investigating the acute (Brünig *et al.*, 2001; Wardle & Poo, 2003; Jovanovic *et al.*, 2004) or chronic (Vicario-Abejón *et al.*, 1998; Yamada *et al.*, 2002) effects of BDNF on GABAergic transmission. mIPSCs were recorded under the same experimental conditions as for those in acutely isolated neurons and described above. In these cultured hippocampal neurons, 10 μM baclofen significantly decreased the frequency of mIPSCs, on average to 58.3 ± 3.6% of the control ($n = 6$; $P < 0.05$), without causing any change in the current amplitude (not shown). In the presence of BDNF (20 ng/mL), 10 μM baclofen again failed to reduce the frequency of mIPSCs, which was 96.5 ± 3.7% of the frequency observed in the presence of BDNF but before the addition of baclofen ($n = 6$; $P = 0.33$). Thus, in both acutely isolated and cultured hippocampal neurons, baclofen reduced mIPSC frequency by a similar extent and this inhibition was reversibly occluded in the presence of BDNF.

BDNF occludes baclofen-induced suppression of eIPSCs in hippocampal CA1 neurons

Next we examined whether BDNF affects the baclofen-induced suppression of evoked inhibitory synaptic transmission in hippocampal slices prepared from P14 rats. Bath application of selective $GABA_B$ receptor agonist, baclofen (1 μM), decreased the mean amplitude of eIPSCs recorded from CA1 pyramidal neurons (which was 47.2 ± 0.8% of the pre-baclofen control; $n = 4$; Fig. 3A and C). This suppression was accompanied by a significant increase in the paired-pulse ratios (PPRs), from 0.88 ± 0.04 to 1.04 ± 0.03 ($P < 0.05$, paired *t*-test), indicating that its locus of action was presynaptic (Fig. 3D).

In the presence of BDNF (50 ng/mL), baclofen reduced the mean amplitude of eIPSCs to 73.3 ± 4.0% of pre-baclofen control, but this suppression was significantly smaller than that in the control condition (Fig. 3C; $n = 3$; $P < 0.01$, unpaired *t*-test). Furthermore, in the presence of BDNF, baclofen did not significantly increase PPRs (from

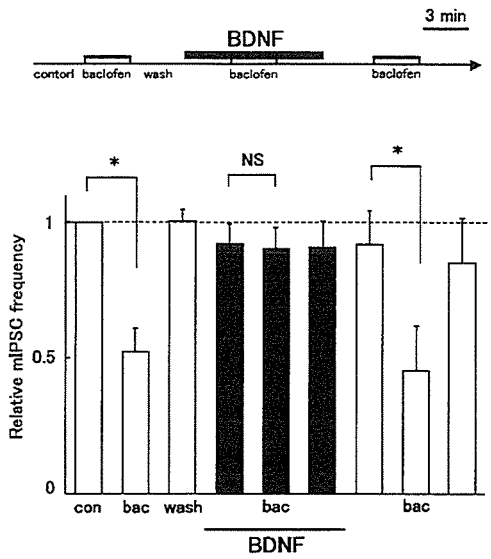

FIG. 2. Brain-derived neurotrophic factor (BDNF) occludes presynaptic $GABA_B$ receptor-mediated inhibition of GABA release in hippocampal CA1 pyramidal neurons isolated from P14 rats. The upper panel shows a schematic illustration of the experimental protocol showing periods of baclofen and BDNF application. Bar graphs show the effects of baclofen on averaged miniature inhibitory postsynaptic currents (mIPSCs) frequency in control conditions (white bars; left side), in the presence of BDNF (black bars; center) and after washout of BDNF (white bars; right side) (*$P < 0.05$; NS, not significant). The mean mIPSC frequency is expressed relative to the initial control frequency. In this, and all subsequent figures, error bars show SEM.

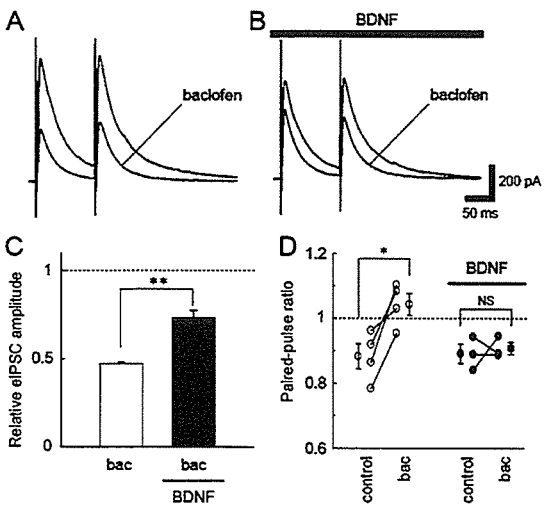

FIG. 3. Brain-derived neurotrophic factor (BDNF) significantly occludes baclofen-induced suppression of evoked inhibitory postsynaptic currents (eIPSCs) in hippocampal CA1 pyramidal neurons at P14 rats. (A, B) Sample traces of IPSC evoked by paired stimuli (100 ms interval) before and during the application of baclofen (1 μM) recorded from CA1 neuron in the control condition (A) and in the presence of BDNF (50 ng/mL; B). Each trace is the average of 10 consecutive IPSCs. (C) Graph showing the effect of baclofen on the averaged amplitude of eIPSCs in control condition ($n = 4$, white bar; left) and in the presence of BDNF ($n = 3$, black bar; right) (**$P < 0.01$). (D) Amplitude ratios of the second to the first IPSCs evoked by paired stimulation are plotted for each cell. Paired values of each neuron are connected by lines. Values were obtained from 10 pulses before and after the baclofen application (*$P < 0.05$, NS; not significant).

0.89 ± 0.03 to 0.91 ± 0.01; $n = 3$; $P = 0.74$; Fig. 3D). These results suggest that BDNF significantly occludes baclofen-induced suppression of eIPSCs in hippocampal slices and its locus of action is presynaptic.

BDNF acts via the presynaptic TrkB receptors

The cellular actions of neurotrophins are mediated via specific high-affinity Trks (Poo, 2001). BDNF specifically binds with high affinity to the TrkB subclass of Trks (Kovalchuk *et al.*, 2004). Hence, we next investigated the role of this receptor tyrosine kinase in the actions of BDNF. In the presence of anti-TrkB polyclonal antibody (TrkB-Ab; 2 μg/mL), baclofen decreased the frequency of mIPSCs to 42.8 ± 11.4% ($n = 5$ from four rats; Fig. 4A), a similar extent of inhibition to that seen with baclofen alone. TrkB-Ab, by itself, increased the basal GABA release somewhat, but this increase was not significant (18.7 ± 15.6%, $n = 5$, $P = 0.08$; Fig. 4A). In the presence of both TrkB-Ab and BDNF (20 ng/mL), baclofen remained effective in inhibiting GABA release, with the frequency of mIPSCs decreasing to 36.4 ± 21.4% of the control frequency in the presence of both TrkB-Ab and BDNF ($n = 5$ from four rats; Fig. 4A).

We next examined the effect of the receptor tyrosine kinase inhibitor, K252a (Tapley *et al.*, 1992). When 150 nM K252a was included in the pipette solution to preferentially block postsynaptic receptor tyrosine kinase, baclofen significantly decreased the frequency of mIPSCs (to 64.3 ± 4.4% of the control; $n = 4$ from three rats; Fig. 4B). In contrast, in the presence of BDNF (20 ng/mL), baclofen had no effect on mIPSCs frequency (which was 108.3 ± 18.3% of the frequency in the presence of BDNF alone; $n = 4$; Fig. 4B).

Thus, BDNF occludes the $GABA_B$ receptor-mediated inhibition of GABA release through the activation of presynaptic TrkBs.

Both pretreatment with the TrkB-Ab or inclusion of K252a in the patch pipette prevented BDNF from reducing the amplitudes of mIPSCs in hippocampal pyramidal neurons isolated from P14 rats (data not shown).

Transduction pathway involved in the occlusion of $GABA_B$ receptor-mediated inhibition of GABA release by BDNF

Subsequent to binding of BDNF to the TrkB receptor, a number of intracellular signaling molecules can be activated, including phospholipase C (PLC)-gamma activation leading to the generation of inositol trisphosphate and diacylglycerol (DAG). BDNF has been shown to stimulate PLC-gamma 1 phosphorylation within 20 s (Widmer *et al.*, 1993). Application of U73122 (5 μM), a membrane-permeant PLC inhibitor (Yule & Williams, 1992), caused a moderate but significant decrease in the frequency of mIPSCs ($P = 0.04$; Fig. 5A). In the continued presence of U73122, baclofen (10 μM) significantly further decreased the frequency of mIPSCs to 63.3 ± 8.0% of that in the presence of U73122 alone ($n = 12$ from nine rats; Fig. 5A). In the presence of both U73122 and BDNF, baclofen caused an almost identical and significant decrease in mIPSCs frequency, to 63.9 ± 14.1% of that observed in the presence of both U73122 and BDNF ($n = 12$ from nine rats; Fig. 5A).

The activation of PLC-gamma would be predicted to activate protein kinase C (PKC) via liberation of intracellular Ca^{2+} and DAG. Indeed, BDNF has been shown to activate PKC in the CNS via this signaling pathway (Segal & Greenberg, 1996). Application of calphostin C (100 nM), a membrane-permeant specific inhibitor of PKC (Kobayashi *et al.*, 1989), by itself, caused a modest but

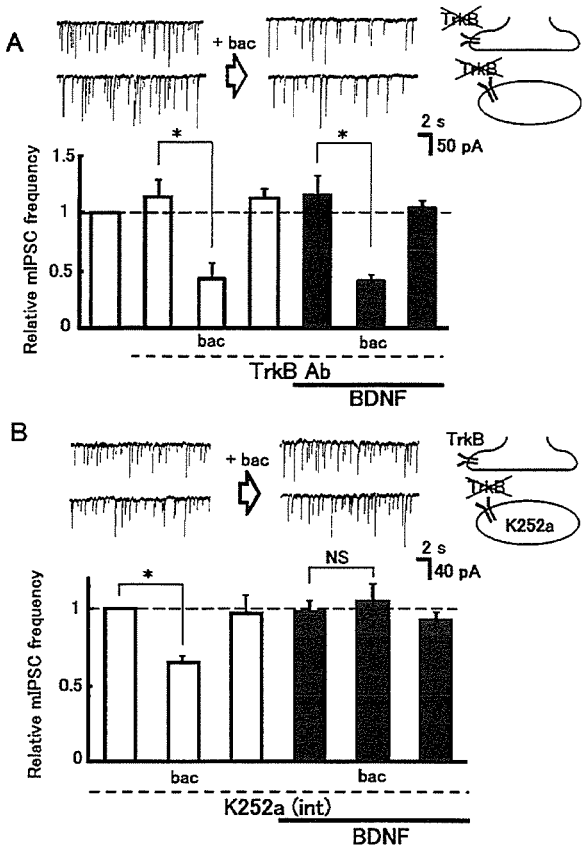

FIG. 4. Brain-derived neurotrophic factor (BDNF) occludes $GABA_B$ receptor-mediated inhibition of GABA release through the activation of presynaptic TrkB tyrosine kinases. (A) Representative traces of mIPSCs in the presence of both BDNF and the TrkB antibody (left) and during additional co-application of baclofen (10 μM; right). The lower bar graph shows the averaged mIPSCs frequency in control conditions (white bars, left), in the presence of TrkB Ab alone (center white bar), in the presence of TrkB Ab and baclofen (white bars, second from right), and following washout of baclofen but in the continued presence of TrkB Ab (white bars, right). The dark bars show the averaged mIPSC frequency in the continued presence of TrkB Ab and BDNF, before (left) during (center) and following (right) baclofen application. All mIPSC frequencies were normalized to that observed in the initial control period. The inset depicts a schematic synapse illustrating that TrkB Ab blocks both pre- and postsynaptic TrkB receptors. (B) Representative traces of mIPSCs in the presence of both K252a and BDNF, and before (left panel) and during (right) the application of 10 μM baclofen. K252a (150 nM) was included in the recording pipettes (inset). The lower bar graphs show the averaged mIPSC frequency all in the continued presence of K252a. The white bars show the averaged mIPSCs frequency recorded before (left), during (center; bac) and after (right) application of baclofen. The dark bars show averaged mIPSC frequency in the additional presence of BDNF before (left), during (center; bac) and after (right) application of baclofen. All mIPSC frequencies were normalized to that observed in the control period in the presence of K252a. The inset depicts a schematic synapse illustrating that K252a loaded in the patch pipette preferentially blocks postsynaptic TrkB receptors. $*P < 0.05$.

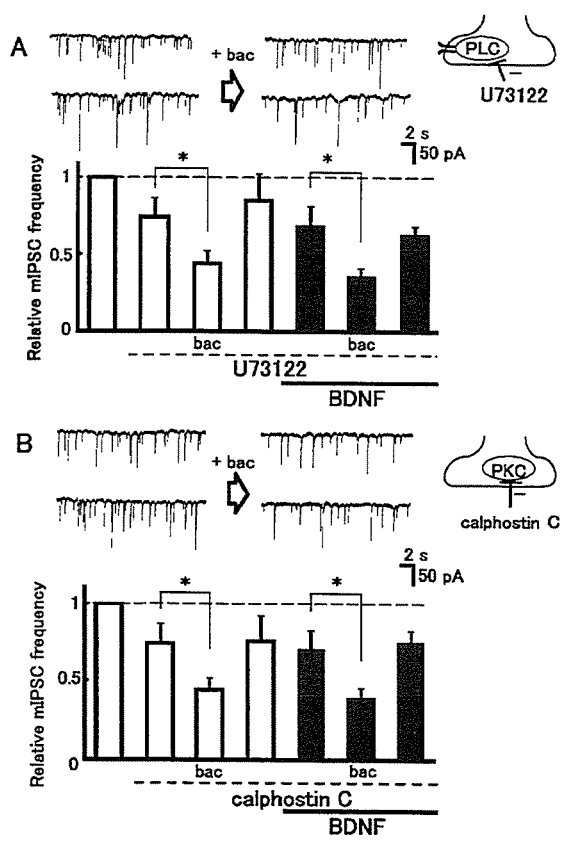

FIG. 5. Transduction pathway involved in the action of brain-derived neurotrophic factor (BDNF) on $GABA_B$ receptor-mediated inhibition of GABA release in rat hippocampal CA1 pyramidal neurons. (A) Representative traces of miniature inhibitory postsynaptic currents (mIPSCs) recorded before (left) and during (right) the application of 10 μM baclofen in the presence of the PLC inhibitor, U73122, and then with both U73122 and BDNF. The lower bar graphs show the effects of baclofen on averaged mIPSC frequency in the presence of U73122 (white bars), and in the presence of both U73122 and BDNF (black bars). The inset depicts a schematic presynaptic terminal with its PLC activity blocked by U73122. (B) Representative traces of mIPSCs recorded before (left) and during (right) the application of 10 μM baclofen in the presence of the specific PKC inhibitor, calphostin C, and then with both calphostin C and BDNF. The lower bar graphs show the effects of baclofen on averaged mIPSC frequency in the presence of calphostin C (white bars), and in the presence of both calphostin C and BDNF (black bars). In both (A) and (B), mIPSC frequencies were normalized to that observed in the initial control period before any drug application (white bars, left). The inset depicts a schematic presynaptic terminal with its PKC activity blocked by calphostin C (Cal C). $*P < 0.05$.

significant decrease in the frequency of mIPSCs ($P = 0.04$; Fig. 5B). In the continued presence of calphostin, baclofen further significantly reduced mIPSC frequency, to 59.6 ± 6.7% of the frequency observed in the presence of calphostin C ($n = 8$ from five rats; Fig. 5B). In the presence of both calphostin C and BDNF, baclofen still significantly decreased mIPSC frequency, to 58.1 ± 7.6% of that in the presence of both calphostin C and BDNF ($n = 8$ from five rats; Fig. 5B).

Together, the above results suggest that BDNF occludes the $GABA_B$ receptor-mediated inhibition of GABA release through the activation of presynaptic TrkB, and subsequent activation of PLC-gamma and PKC.

Developmental change in the occlusion of $GABA_B$ receptor-mediated inhibition of GABA release in rat hippocampal CA1 pyramidal neurons by BDNF

The modulation of $GABA_A$ responses in hippocampal pyramidal neurons by BDNF changes over development, from a reversible potentiation (at P6) to a sustained suppression (at P14; Mizoguchi *et al.*, 2003a). It was therefore of interest to investigate whether the

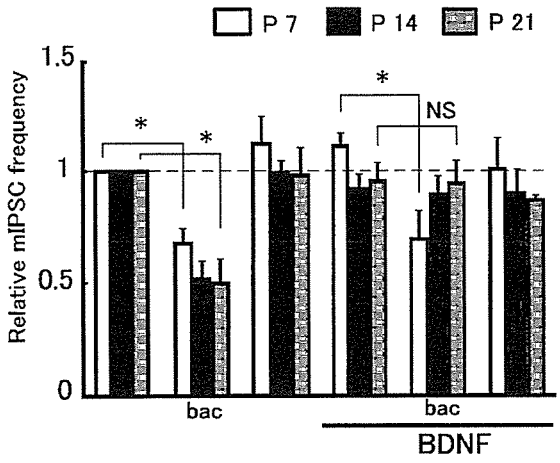

FIG. 6. Developmental change in the occlusion of $GABA_B$ receptor-mediated inhibition of GABA release in rat hippocampal CA1 pyramidal neurons by brain-derived neurotrophic factor (BDNF). The bar graphs show the effects of baclofen on averaged miniature inhibitory postsynaptic current (mIPSC) frequency before and during the application of BDNF, recorded in neurons isolated from P7 (white bars), P14 (black bars) and P21 (gray bars) rats. $*P < 0.05$.

actions of BDNF on $GABA_B$ receptors also changed during development.

Hippocampal CA1 pyramidal neurons were acutely isolated from developing rats at two additional ages, P7 and P21. In pyramidal neurons isolated from both these ages, 10 μM baclofen significantly decreased the frequency of mIPSCs, without causing any change in the current amplitude (not shown). Mean mIPSC frequency was decreased to 66.1 ± 6.4% of the control ($n = 8$ from seven rats; $P = 0.007$) in neurons from P7 rats, and to 50.1 ± 11.1% of the control ($n = 6$ from four rats; $P = 0.01$) in neurons from P21 rats. This was similar to the baclofen response in neurons from P14 rats (Fig. 6). At all ages, the averaged mIPSC frequency recovered back to control values within 3 min of washing out baclofen (Fig. 6).

In P21 neurons, in the presence of BDNF (20 ng/mL), 10 μM baclofen failed to cause any reduction in the frequency of mIPSCs, which was 97.3 ± 8.2% of the frequency in the presence of BDNF alone, as was observed in P14 rats ($n = 6$; Fig. 6). In contrast, in pyramidal neurons isolated from P7 rats, BDNF (20 ng/mL) failed to occlude the ability of baclofen to inhibit GABA release, with mIPSC frequency being 63.7 ± 9.2% of that observed in the presence of BDNF alone ($n = 8$, $P = 0.012$) and similar to the baclofen response prior to BDNF application (Fig. 6). These results indicate that the ability of BDNF to occlude the $GABA_B$ receptor-mediated inhibition of GABA release develops between P7 and P14.

PKC activation also occludes $GABA_B$ receptor-mediated inhibition of GABA release

It has previously been reported that in CA1 neurons in hippocampal slices from 2–3-week-old rats, activation of PKC with the phorbol ester, PDBu, reduces the $GABA_B$ receptor-mediated inhibition of mIPSC frequency (Jarolimek & Misgeld, 1997). We examined whether a similar effect was observed for dissociated CA1 neurons from P14 and P7 rats. Pretreatment of neurons from P14 rats with PDBu (1 μM), which binds to the DAG binding site of PKC, caused a modest but non-significant increase in mIPSC frequency and occluded any significant baclofen-induced inhibition of mIPSCs frequency

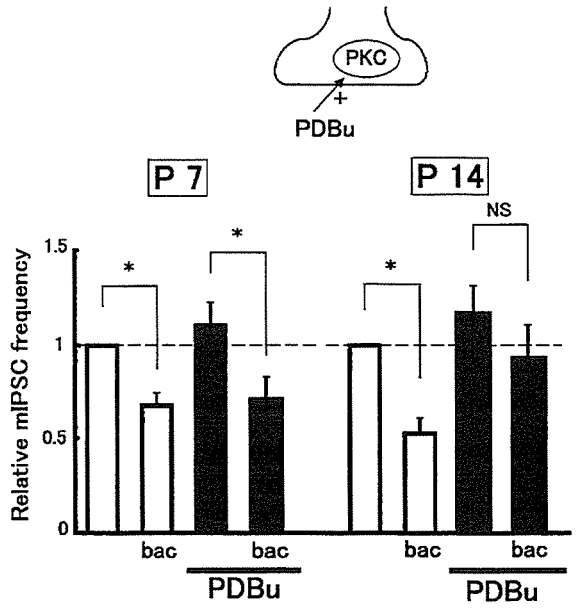

FIG. 7. Protein kinase C (PKC) activation occludes the $GABA_B$ receptor-mediated inhibition of GABA release in hippocampal CA1 pyramidal neurons isolated from P14, but not P7 rats. The bar graphs show the effects of baclofen on averaged miniature inhibitory postsynaptic currents (mIPSCs) frequency before (white bars) and in the continued presence of the PKC activator, phorbol-12,13-dibutyrate (PDBu, black bars) in neurons isolated from P7 (left side) and P14 (right side) rats. mIPSC frequencies were normalized to that observed in the initial control period before any drug application, as indicated. The inset depicts a schematic presynaptic terminal with its PKC being activated by PDBu. $*P < 0.05$.

(which was 83.6 ± 10.8% of the frequency in the presence of PDBu alone; $n = 8$ from six rats; Fig. 7). In contrast, PDBu (1 μM) pretreatment of neurons isolated from P7 rats failed to affect the baclofen response, with the frequency of mIPSCs being reduced to 58.2 ± 5.7% of that observed in the presence of PDBu alone ($n = 5$ from three rats; Fig. 7). At P7, pretreatment with PDBu also caused a modest but non-significant increase in mIPSC frequency.

Discussion

In the present study, we demonstrated that BDNF significantly occludes baclofen-induced suppression of $GABA_A$ receptor-mediated transmissions in each of the preparations, including hippocampal CA1 pyramidal neurons isolated from P14 and P21 rats, cultured hippocampal pyramidal neurons and hippocampal slices prepared from P14 rats. We also showed that occlusive action of BDNF was caused by the activation of the presynaptic TrkB and subsequent activation of PLC-gamma and PKC. The BDNF occlusion of baclofen-induced inhibition of GABA release was absent in neurons isolated from P7 rats, indicating that this response develops between the first and second postnatal week.

In the rat hippocampal CA1 region, the high-affinity TrkB receptors are located on the somata and dendrites of pyramidal neurons, and dense labeling is also found on the axon terminals of GABAergic neurons (Drake *et al.*, 1999), with their expression levels reaching closer to adult level by P5 (Fryer *et al.*, 1996). Activation of these TrkB receptors by BDNF results in activation of PLC-gamma, liberation of DAG and intracellular Ca^{2+}, and subsequent activation of PKC (Segal & Greenberg, 1996). The acute effects of BDNF on